

Categorization Methodology for Skin Color Images into Pre-Defined Color Scales

By

Parisa Mohammadalizadeh

M.Sc. (Electrical Engineering), Tabriz University, 2014

Thesis Submitted in Partial Fulfillment of the
Requirements for the Degree of
Master of Applied Science

in the
School of Mechatronics Systems Engineering
Faculty of Applied Science

© Parisa Mohammadalizadeh 2019
SIMON FRASER UNIVERSITY
Fall 2019

Copyright in this work rests with the author. Please ensure that any reproduction or re-use is done in accordance with the relevant national copyright legislation.

Approval

Name: Parisa Mohammadalizadeh

Degree: Master of Applied Science

Title: Categorization Methodology for Skin Color Images into Pre-defined Color Scales

Examining Committee:

Chair: Mehrdad Moallem
Professor

Farid Golnaraghi
Senior Supervisor
Professor

Amr Marzouk
Supervisor
Lecturer

Mohammad Narimani
Internal Examiner
Lecturer

Date Defended/Approved: 09 09, 2019

Abstract

The ability to classify skin color based on images from bare skin is highly sought after in various industries and professions, including dermatology, cosmetics, skincare products, laser-based therapies, etc. The focus of the present research work is on designing an algorithm capable of classifying images of various skin colors utilizing the Fitzpatrick and cosmetic brand skin color scales. The images are taken from a skin area by any camera, including a smartphone camera.

In this study, two different methods are employed to classify a query image into a set of reference images. Both methods introduced here are among the most commonly used approaches for comparing two image histograms and defining a Difference Index (DI). The application of the proposed algorithms is not limited to the classification of skin colors. These algorithms can be applied in painting industry for building interiors, developing apps for assisting people who are color-blind, etc.

Keywords: Skin color, Image classification, Histogram matching.

*To my father for his endless support,
to my mother for being my first teacher,
to my husband for his continuous
encourage and
to my sister and brother for believing me.*

Acknowledgments

I would like to express my sincere appreciation to my senior supervisor, Dr. Farid Golnaraghi for his continuous support and guidance. As my senior supervisor, he has taught me more than I could ever give him credit for here. He has shown me, by his example, what a good scientist (and person) should be.

Nobody has been more important to me in the pursuit of my thesis than the members of my family. I would like to thank my parents; whose love and guidance are with me regardless of where they are. Most importantly, I owe my deepest gratitude to my husband for his continuous support and encouragement and passion throughout my academic career.

Last but not least, my special thanks to Dr. Amr Marzouk for his time, knowledge and fruitful discussion on this work.

Table of Contents

Approval.....	ii
Abstract	iii
Dedication.....	iv
Acknowledgments	v
List of Figures	viii
List of Tables	x
Chapter 1. Introduction	1
1.1. Background and Overview	1
1.1.1. Color	1
1.1.2. Impact of Radiations on Skin	2
1.1.3. Skin Color Measures.....	3
1.2. Current Technologies for Skin Color Classification	7
1.2.1. Challenges in Reflectance Spectrophotometer	8
1.3. Motivations for the research	8
1.4. Research Objectives	9
1.5. Accomplishments.....	10
Chapter 2. General Study of Image Classification Methodologies	11
2.1. Introduction	11
2.2. Introduction to Color Spaces	12
2.2.1. RGB Color Space	12
2.2.2. La* b* Color Space.....	14
2.2.3. HSV Color Space	15
2.3. Image histogram matching techniques	17
2.3.1. Conventional Histogram Intersection (HI) Method	17
2.3.2. Merged Palette Histogram Matching (MPHM) Method	18
2.3.3. Modified Color Histogram Method	19
2.4. Distance measurements technique.....	23
2.4.1. Euclidean distance.....	23
2.4.2. City Block Distance	24
2.4.3. Chess Board Distance.....	24
2.5. Validation Set	25
2.5.1. Generalized extreme value distribution	25
Chapter 3. Experimental Results for Skin Color Classification.....	27
3.1. Introduction	27

3.2. Validation Set Generation Using Extreme Value Distribution	28
3.2.1. Organized Image Creation Using RGB Color Histograms	29
3.2.2. Application of GEVD on Fitzpatrick scale	30
3.2.3. Application of GEVD on Dior Skin Color Palette	30
3.3. Euclidean Distance Application for Image Retrieval.....	37
3.4. Application of Color Histogram Matching for Image Retrieval.....	40
3.4.1. The Fitzpatrick Image Retrieval Using Modified Color Histogram Matching	40
3.4.2. Dior Palette Image Retrieval Using Modified Color Histogram Matching	44
3.5. Application of Euclidean Distance and Modified Histogram matching methods on Real Skin Image-Set	47
3.6. Experimental Results on Skin Phantoms for Dior Skin Palette	52
3.7. Conclusions	55
Chapter 4. Conclusion & Future Works	56
References.....	58

List of Figures

Figure 1.1: Felix von Lanchan skin color scale [18].	4
Figure 1.2 Range of colors by the Fitzpatrick scale	5
Figure 1.3: Range of skin color by NIS chart	6
Figure 1.4: Twelve shades of Dior skin palette	7
Figure 2.1: RGB Color cube.	13
Figure 2.2: RGB color and their corresponding intensity	13
Figure 2.3: $L^* a^* b^*$ color model [36].	14
Figure 2.4: A sample image in (a) RGB color space, (b) $L^* a^* b^*$ color space.	15
Figure 2.5: HSV color model	16
Figure 2.6: A sample image in (a) RGB color space, (b) HSV color space	16
Figure 2.7: An example for the problem with the conventional HI algorithm	20
Figure 2.8: The solution for the problem with the conventional HI algorithm, using Modified Histogram matching method.	21
Figure 2.9: Two Query images histogram compared to a sample reference image	22
Figure 2.10. Modified single bar histogram using Gaussian distribution	22
Figure 2.11: PDF of the extreme value distribution.	26
Figure 3.1: Perturbed Fitzpatrick scale.	31
Figure 3.2: Color histograms for the Fitzpatrick scale reference	32
Figure 3.3: Perturbed reference image histograms for the Fitzpatrick scale.	33
Figure 3.4: Perturbed Dior skin palette.	34
Figure 3.5: Color histograms for Dior cosmetic palette reference images	35
Figure 3.6: Perturbed reference image histograms for Dior skin palette	36
Figure 3.7. Fitzpatrick scale image retrieval, using “Euclidean distance”	38
Figure 3.8. Dior cosmetic palette image retrieval using “Euclidean distance”	39
Figure 3.9. Gaussian distribution histograms for the Fitzpatrick scale reference images	41
Figure 3.10. The Fitzpatrick scale image retrieval using “single bar Image Histogram”	42
Figure 3.11. The Fitzpatrick scale image retrieval using “Modified histogram matching” method	43
Figure 3.12. Gaussian distribution histograms for Dior cosmetic palette reference image	45
Figure 3.13. Dior cosmetic palette image retrieval using “single bar Image Histogram”	46
Figure 3.14. Dior cosmetic palette image retrieval using “Modified Histogram Matching.”	47

Figure 3.15: Dior skin foundation shades classification based on the Dior palette 53
Figure 3.16: Modified Dior skin foundation shades classification based on the Dior palette 54

List of Tables

Table 1.1: Detailed Fitzpatrick skin scale	6
Table 3.1: Fitzpatrick Color Codes	28
Table 3.2: The Fitzpatrick real skin image classification Using “Pixel-by-pixel” algorithm	48
Table 3.3: Fitzpatrick real skin image classification using “Modified histogram matching.”	49
Table 3.4: Dior palette real skin image classification Using “Pixel-by-pixel” method	50
Table 3.5: Real skin Dior palette classification using “Modified histogram matching”	51

Chapter 1. Introduction

The Skin, comprising almost 16% of the body mass, is considered as the largest organ [1]. Human skin exists in a wide range of various colors, ranging from white to brown to black. This is due to the presence of a chemically inert pigment called melanin, which is produced deep inside the skin but is shown as a mosaic at the surface of the body. Melanin is therefore responsible for the most striking polymorphic traits of humans and for the most obvious and thoroughly discussed aspect of human geographical variability: skin color. Besides its role in defining ethnicity, melanin plays an essential role in defending the body against harmful Ultra Violet (UV) rays and other environmental challenges. From a clinical perspective, insufficient protection from sunlight has a major impact on human health. It is quite impossible to completely avoid the UV radiations as the sun is an inevitable part of our life. It is shown that more melanin means higher skin protection [2].

Dermatology is one of the branches of medical science which deals with diagnosis and treatment of skin disorders. Most dermatological diseases are due to environmental factors such as temperature, sunlight, humidity, etc. Skin color is one of the most important features which is used by health care professionals in dermatology for diagnosing different diseases or injuries, where the overall skin health is linked to oxygenation, tissue perfusion, nutritional status, and injury [3]. Clinicians make decisions based on changes in skin color. They evaluate pressure points for early signs of skin breakdown and assess existing wounds for color changes that might indicate healing, worsening, or infection [1], [4].

1.1. Background and Overview

Considering the significance of skin color, understanding its concept, and the available scales for classifying, it plays a key role in preventing many skin disorders [5], [6].

1.1.1. Color

Light is made up of different wavelengths; each is representing a particular color. The colors we see in visible light are reflected by (or transmitted through) objects and have a particular wavelength, ranging from 400 nm (violet) to 700 nm (red), which is captured by the eyes and is interpreted by the brain as a specified color. Different objects have different colors because of

their capacity to absorb or reflect certain wavelengths. The retina is the key sensory system in the eye, allowing our brain to distinguish different colors. Colors have three properties: hue, brightness, and saturation, as defined below [7]:

Hue- The hue of a color refers to what is frequently known as “color”. For instance, all red colors have a similar hue value, whether they are light, dark, or intense.

Saturation- The saturation of a color refers to the purity or intensity of the color. When a color is fully saturated, it is deep and brilliant. Accordingly, by decreasing the saturation, the color gets paled until it finally turns to neutral. The “grayness” will increase by lowering the saturation and also the color will be more washed out.

Brightness- The level of darkness or lightness of a color is identified by its brightness. Zero brightness in any color means black, regardless of its hue or saturation. Brightness ranges from 0-100%.

1.1.2. Impact of Radiations on Skin

There are many types of electromagnetic radiations that are used in various therapies and treatments. Solar radiation that reaches the earth’s surface is primarily non-ionizing (UV, visible light, and infrared radiations). Radio waves have large wavelengths but low frequencies and energy, whereas gamma rays have small wavelengths but high energy level. The radiofrequency energy is applied in different therapeutic and cosmetic approaches. Infrared radiation is used as a skin treatment purpose in dermatology. Despite the therapeutic application of these radiations, several skin damages have been reported [8].

Skin complexion is one of the most significant determinants of radiation sensitivity and skin cancer risk. It has been proven that categorization of skin color into pre-defined scales helps dermatologists to prevent skin-related disorders [9]. Human skin is categorized into six classes by Fitzpatrick’s Scale. This Scale has been widely used for estimating skin sensitivity to UV, psoralen, and ultraviolet A (PUVA), and laser treatment doses [10], [11], [12]. Skin color classification would be helpful in these treatment processes.

1.1.3. Skin Color Measures

The appearance of human skin is a major parameter in both clinical studies and cosmetic industry. Skin color can be used to explore the susceptibility to the development of skin cancer [13], [14]. Changes in skin color have been used as a measure to characterize erythema [15], [16]. Monitoring the skin color variations is a significant clinical basis for the diagnosis of cutaneous malignant melanoma and benign nevi [21].

Skin color scales have been widely used in assessing the color of skin. There are three well-known skin color scales used in the industry and academia: Felix von Luschan, Fitzpatrick, and New Immigrant Survey (NIS). These scales are described in detail in the following subsections.

The best facial structure can look unbalanced by a flawed skin type. Foundations have been a popular solution to address this problem so far. Every cosmetic brand owns a specific skin shade palette for their foundation products. Finding a perfect foundation match is one of the greatest challenges in the beauty world. Since this study aims to provide a solution to find the best match for any skin type based on the image of the skin, a cosmetic brand skin palette has been chosen to apply in this study. The palette is presented in the following subsections.

1.1.3.1. Felix. Von Luschan Scale

In the late 1880s, German anthropologist Felix von Luschan proposed a new skin color scale that would allow for classification of skin color data. This scale became known as Felix von Luschan's Chromatic scale, which is composed of a set of 36 colored glass tiles. This scale became the standard technological system for skin color data for the field study of anthropology until the 1950s [18]. The colors in this scale are reproduced in Figure 1.1.

	1	10			19	28	
	2	11			20	29	
	3	12			21	30	
	4	13			22	31	
	5	14			23	32	
	6	15			24	33	
	7	16			25	34	
	8	17			26	35	
	9	18			27	36	

Figure 1.1: Felix von Lunhan skin color scale [18].

1.1.3.2. Fitzpatrick Scale

In 1975, Thomas B. Fitzpatrick was the first researcher to develop skin scale to assess human skin color and sun exposure reactions in terms of burning and tanning. It has been proven that the Fitzpatrick skin scale has remarkable diagnostic and salutary significance [19].

Previously, the Fitzpatrick scale classified skin into three types, based on his research on the effect of sunscreen on the tanning or burning of the skin [20]. He distributed skin responses of fair-skinned Australians who participated in his study of midday sun exposure into three main sun reactive categories [6].

- Skin phototype I: those who burn easily and do not tan at all
- Skin phototype II: those who burn easily and tan with difficulty (freckled and often red-haired individuals)
- Skin phototype III: those who burn moderately, had immediate pigment darkening reactions, and tan moderately after about 60 minutes of midday sun exposure.

Fitzpatrick's original skin scale I, II, and III became well accepted and were adopted in dermatology for phototherapy of skin diseases. In 1972, the US FDA adopted this classification for the evaluation of sun protection factor (SPF) values of sunscreens [6].

Through the numerical classifications of human skin types, an individual's UV tolerance level [21] may be assessed. The Fitzpatrick skin Scale help physicians to recognize a person's risk of getting sunburn and, by extension, the risk of contracting skin cancer [19].

The current Fitzpatrick skin type classification [20] specifies six different skin colors. The range of Fitzpatrick scale starts from very fair (skin type I) to very dark (skin type VI) depending on if the patient burns or tans at the first average sun exposure. Figure 1.2 shows the range of colors for human skin as described by Fitzpatrick scale. Table 1.1 shows detailed skin classification by Fitzpatrick scale.

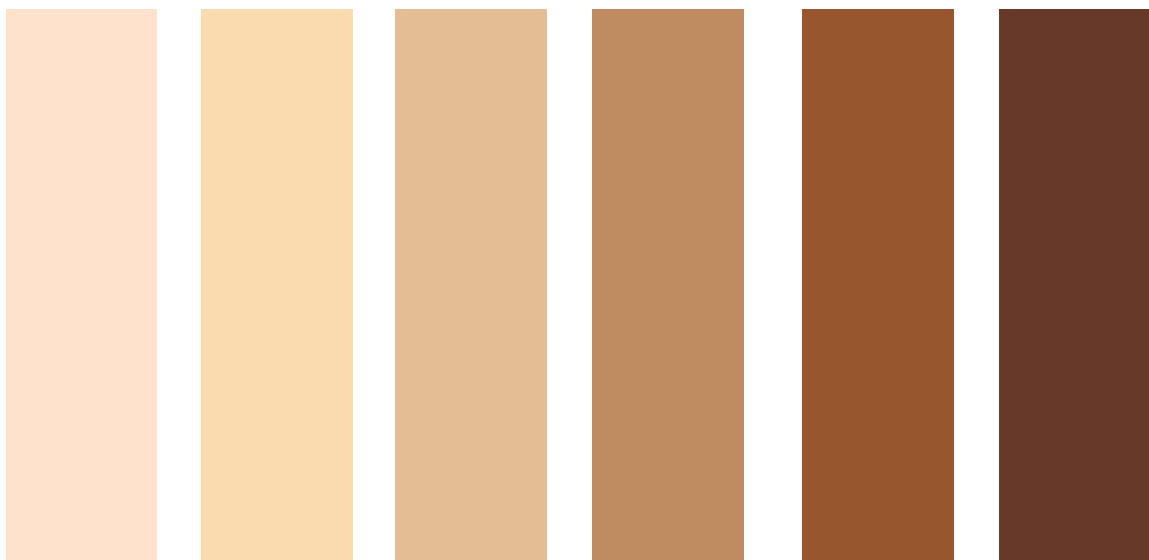


Figure 1.2 Range of colors by the Fitzpatrick scale

Table 1.1: Detailed Fitzpatrick skin scale

Skin phototype	Typical Features	Tanning ability
I	Pale white skin, blue/hazel eyes, blond/red hair	Always burns does not tan
II	Fair skin, blue eyes	Burns easily, tans poorly
III	Darker white skin	Tans after the initial burn
IV	Light brown skin	Burns minimally, tans easily
V	Brown skin	Rarely burns, tans darkly easily
VI	Dark brown or black skin	Never burns, tan darkly

1.1.3.3. NIS Scale

The New Immigrant Survey (NIS) measures skin color, based on an idea originally developed by Massey, Charles, Lundy, and Fischer [22]. This scale is an eleven-point scale, ranging from zero to 10. Zero shows the total absence of color, and ten shows the darkest skin. The range of skin color corresponding to the ranges 1 to 10 on the Massey and Martin Skin Color Scale are represented in a chart, with each point demonstrated by a hand of identical form but differing in color. The Scale was constructed with assistance from a graphic designer [23]. Figure 1.3 shows the NIS skin chart.

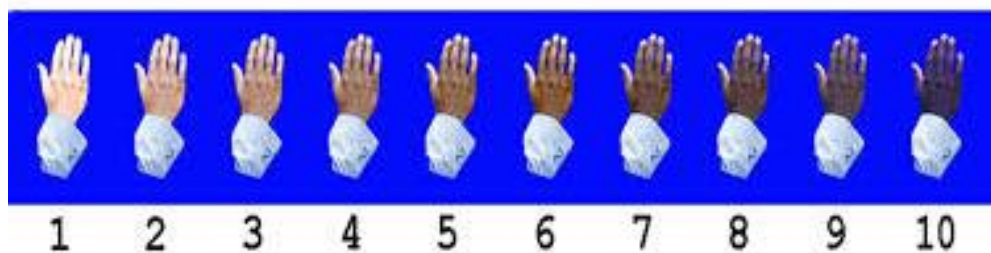


Figure 1.3: Range of skin color by NIS chart

1.1.3.4. Dior Foundation skin Palette

Skin color palettes provide customers the available skin shade foundations to select the best match for their skin type. Among the cosmetic brands, the Christian Dior brand [24] is selected to be implemented in this study. This brand provides a high number of skin shades for its foundation products which meet the requirements of our study. The twelve shades set for skin foundation by Dior brand is demonstrated in Figure 1.4.

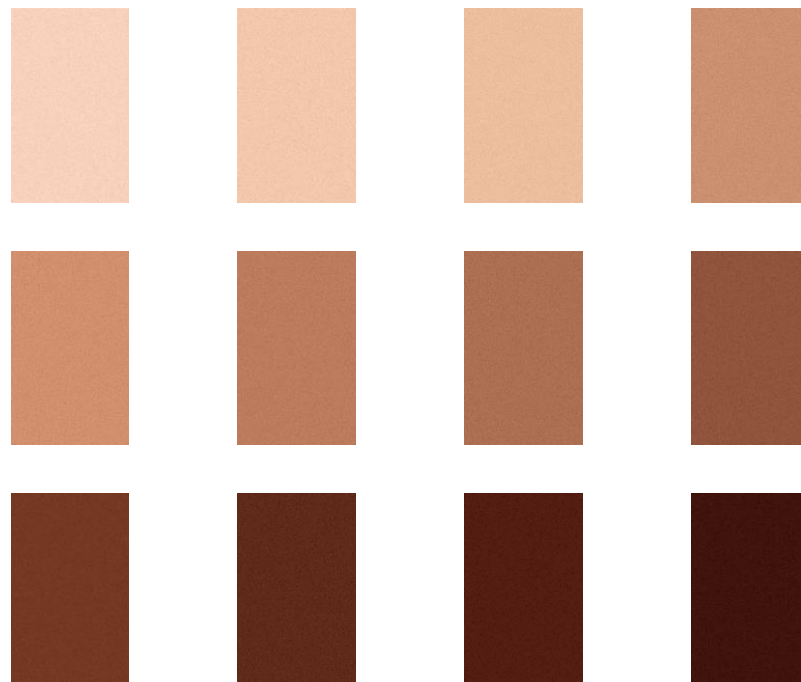


Figure 1.4: Twelve shades of Dior skin palette

1.2. Current Technologies for Skin Color Classification

Skin reflectance spectrophotometer was developed for detection of color variations in dermatological disorders [25]. Diffuse reflectance spectroscopy (DRS), as a non-invasive method, is considered to be the standard for objective quantitative measurement of skin color. It

has been tested in the cosmetics industry as well as by scientists investigating ultraviolet ray exposure to the skin.

The investigator uses the instrument to illuminate the area of interest by a direct light with specific wavelengths. Then, the wavelength(s) and intensity of light reflected from the skin back to the instrument's sensors are measured to identify the color. DRS records reflectance values from colored surfaces and provides instrument operators with color measurements [1], [26].

1.2.1. Challenges in Reflectance Spectrophotometer

Alternations of tissue thickness, composition, surface structure, texture, and vascularity, as well as the concentration and distribution of chromophores in the interested surface, may all contribute to the optical properties of the substance. At this moment, these factors can directly affect the outcome of reflectance spectrometer.

Besides, the final cost of this device in the market is too expensive. Spectrophotometers vary in cost from approximately \$5,000 to \$15,000 US per unit, depending on model capabilities, with further costs depending on the software, accessory hardware, or warranty/service plan [1], [26]. On the contrary, classification of human skin color based on the image of the areas of interest is totally free of charge.

1.3. Motivations for the research

Radiation exposure may cause severe skin changes that significantly interfere with a person's quality of life [27]. Detection of skin color will help dermatologists and medical practitioners to assess skin type and diagnose possible skin damages caused by radiotherapy or other laser treatments.

Color assessment methods may be categorized as either subjective or objective. Subjective assessment is based on an individual's interpretation of stimuli, while objective measurements are based strictly on the phenomenon of interest and not subject to judgment or bias. In the past, most skin color assessment has been performed subjectively through the use of visual inspection, comparative color tiles or laminated color cards, written skin-typing guidelines for comparative classification, or by way of qualitative visual estimation by individuals who have received varying levels of training [28], [29]. The accuracy of these subjective measures for the

assessment of skin color could be considered uncertain at best, and the repeatability is dependent on a combination of factors, including ease of scale use, degree of rater training, and physical influences. Using an objective method which can detect the color of skin (or any other area) will provide the real color of the area regardless of any interpretation for the color detection.

Our study focuses on designing a technique to classify various skin colors into pre-defined categories. Handheld devices made particularly for this purpose will require efficient and robust algorithms in order to classify skin color in real-time.

The machine learning algorithms could be a good way to apply on this thesis to classify the skin images, however there were not available labeled image data set for any of the implemented skin scales of this study. Hence, we aimed to meet the goal of this research based on algorithms which are accurate enough and don't need any data set.

1.4. Research Objectives

The primary goal of this study is to categorize human skin color in a desired set of colors. The Fitzpatrick scale [9] and a color palette from Dior [23], a cosmetic brand, were selected as the pre-defined reference categories in this study. The main challenge, considering an unsupervised system application, was the lack of available dataset for this study in this study.

Images of skin colors are unique in the sense that most of the pixels pertain to one color, and there are not spatial variations that can assist in defining a feature. As such, many of the available image recognition algorithms that rely on spatial-dependent features cannot be directly applied to this problem. In this study, two different methods are employed to classify a query image into a set of reference scales. The first method is the modified color histogram matching (MCHM). This method is independent of the spatial distribution of pixels in an image and is perfectly suitable for analysis on skin color images. The modifications proposed in this research to the conventional histogram matching method are based on the premise that the reference images are monotone-color. Using the MCHM method, the calculated difference indices (DIs) are more meaningful and show the similarities/differences. DI is the factor for assessing the difference between two images. The second method is based on the Euclidean distance (ED) between a query image and the reference images. ED is a simple and straight-forward method to measure

the distance between two vectors. This method is robust and depends on the spatial distribution of pixels. Both methods introduced here are among the most commonly used approaches for comparing two images and defining a DI.

In order to validate the introduced methods, a set of query images is created by systematically perturbing the reference images. The level of perturbation is controlled in a way that the resulting image is sufficiently similar to the original reference image. This way, the correct classification result would be known, and the success rate of the introduced methods can be readily examined. Also, the introduced algorithms are applied to real skin images obtained from an online resource [30]. One challenge for the algorithms is to differentiate between closely similar skin colors which human eye may not be capable of detecting. This was observed in the real data set, and both algorithms successfully handled the challenge.

1.5. Accomplishments

The proposed algorithms have been successfully tested on both a well-formed validation set and real skin images. The tests are done based on selected reference images. Fitzpatrick scale and a set of twelve images from Dior cosmetic palette are selected as the reference images in this study.

The required validation set for this study is created by perturbing the selected reference images. The success rate of each algorithm can be determined by comparing the two sets of images (perturbed reference images and original reference images). Both MCHM and ED methods provided accurate results for the classification.

The algorithms are also examined on real skin images in the second part of the study. These images are cropped from portrait images of different human races published in an online resource [30]. All images are classified based on pre-defined reference images. The results of the applied methods are highly matched in either Fitzpatrick scale or Dior cosmetic palette.

Chapter 2. General Study of Image Classification Methodologies

2.1. Introduction

This chapter focuses on the main features that contribute to the comparison of images. Color space selection, color histogram matching methods, image distance calculation are all among the features which play major role to compare a set of images.

There are several color spaces available in color studies. Some of the most leading color spaces which are known in image processing and color analysis have been introduced in this chapter.

Next, various approaches are introduced for comparing color histogram. Conventional Histogram Intersection (HI), Merged Palette Histogram Matching (MPHM) and Modified Histogram Matching method are all demonstrated in this section.

Histogram-based image matching algorithms are spatially independent image retrieval techniques for measuring the similarity in image contents via their histograms between a query image and any images in the data-set. An image retrieval system is a computer system for browsing, searching, and retrieving images from a database of images. It has been shown that introduced image histogram matching algorithms have a restriction for monotone color images comparison. In this chapter, this constraint is presented, and its solution is provided by applying a similarity weight using Gaussian distribution on our monotone color image histograms.

Calculation of the distance between two images is another approach to retrieve a color image from a set of reference images. This approach is spatial dependent where all the spatial features of the image content (shape, texture, etc.) directly affect the image retrieval result. The available methods are all covered in next section of this chapter. Due to the simplicity and high accuracy of Euclidean distance method, it is applied in this study to calculate the distance between the query image and a pre-defined reference image.

The chosen algorithms for retrieving a query image from a set of reference images should be tested to validate their accuracy. Therefore, a validation set is required to confirm whether the algorithms act accurately. The required validation set is established by perturbing the reference images. This topic is illustrated in detail in the last section of this chapter.

2.2. Introduction to Color Spaces

The most widely accepted model for color quantification was established by the Commission Internationale d'Eclairage in 1976 and is described as a color space or a three-dimensional geometric model that represents color numerically. A color space is a specific arrangement of colors, which, in combination with physical device profiling, allows for the reproducible representation of colors in both digital and analog formats. While color is reproduced in another device, the color space validates the details for shadow, highlight or color saturation are fully preserved [31]. RGB, L*a*b* and HSV are three key color spaces which have a direct impact on color comparison studies.

Considering the different conditions of the environment which the images are taken, we should think of applying such a color space that is capable of ignoring the noises as much as possible. To be more precise, the chosen color spaces must be able to carry the lowest amount of noise. Among the available color spaces, L*A*B* and HSV are the two most used color spaces which carry the minimum amount of noise.

A comprehensive study was conducted in [32] between two L*A*B* and HSV color spaces. These two color spaces are the most commonly implemented in studies of the color image. Both color spaces are good enough at removing noises compared to the other available color spaces. However, the experimental results in this study demonstrate that neither HSV nor L*A*B* color spaces provide valid results for monotone color images [32].

2.2.1. RGB Color Space

The visible light range is composed of electromagnetic wavelengths ranging from 400 to 700 nm. Most display systems use three channels to render the color image, Red, Green, and Blue in RGB color spaces [33]. The RGB color cube has been demonstrated in Figure 2.1.

Every pixel of an image assumes a certain color. There are many color spaces to represent the numerical values of the colors. RGB color space shows the color of each pixel based on three different colors, Red, Green and Blue. The intensity of these colors is shown with integer numbers starting from 0 to 255. Figure 2.2 shows these colors and their intensity.

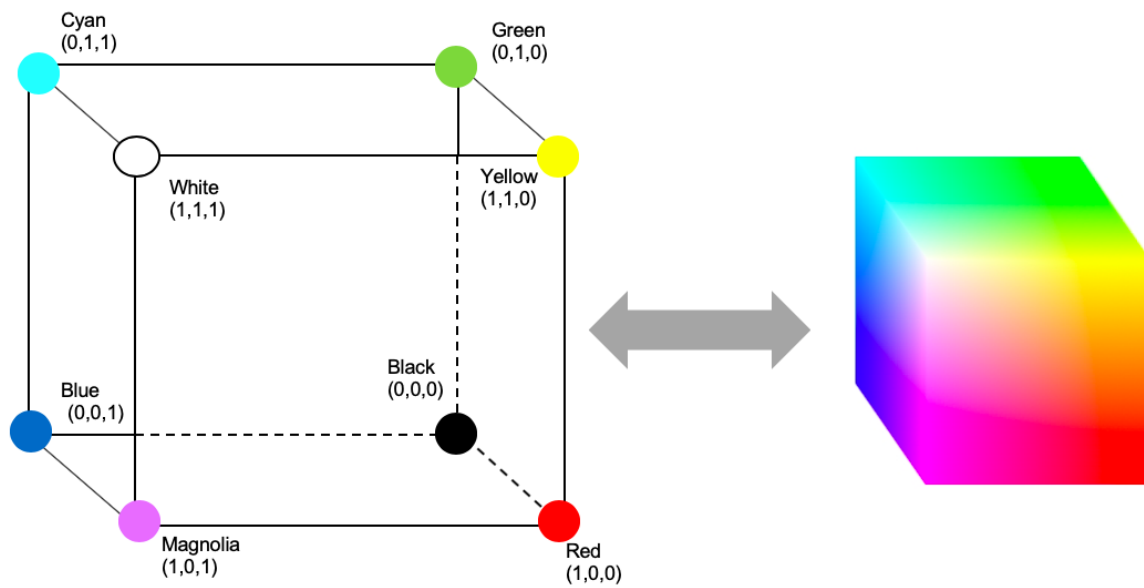


Figure 2.1: RGB Color cube.

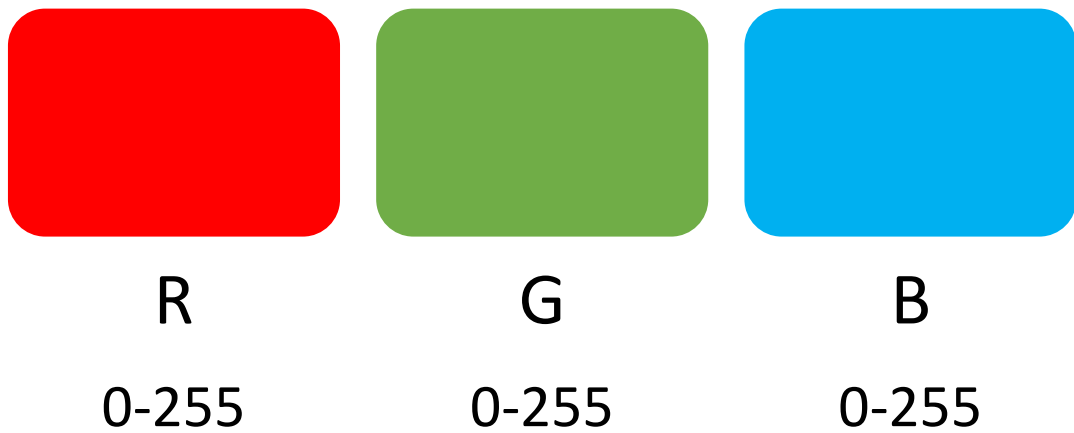


Figure 2.2: RGB color and their corresponding intensity

As images can be represented in matrices, every image is comprised of three different matrices for Red, Green and Blue colors. For an image in RGB color space:

$$R_{m \times n} = \begin{bmatrix} r_1 & \cdots & r_n \\ \vdots & \ddots & \vdots \\ r_m & \cdots & r_{m \times n} \end{bmatrix} \quad G_{m \times n} = \begin{bmatrix} G_1 & \cdots & G_n \\ \vdots & \ddots & \vdots \\ G_m & \cdots & G_{m \times n} \end{bmatrix} \quad B_{m \times n} = \begin{bmatrix} B_1 & \cdots & B_n \\ \vdots & \ddots & \vdots \\ B_m & \cdots & B_{m \times n} \end{bmatrix}$$

2.2.2. $L^* a^* b^*$ Color Space

In the $L^* a^* b^*$ color space, Value L^* represents lightness/darkness and extends from 0 (black) to 100 (white). Value a^* represents the redness/greenness axis; positive a^* is red and negative a^* is green. Value b^* represents the yellowness/blueness axis; positive b^* is yellow and negative b^* is blue. There are no specific numerical limits for a^* and b^* [34], [35], [33]. The sphere model for $L^* a^* b^*$ space is shown in Figure 2.3. A sample image in $L^* a^* b^*$ and RGB color spaces are shown in Figure 2.4.

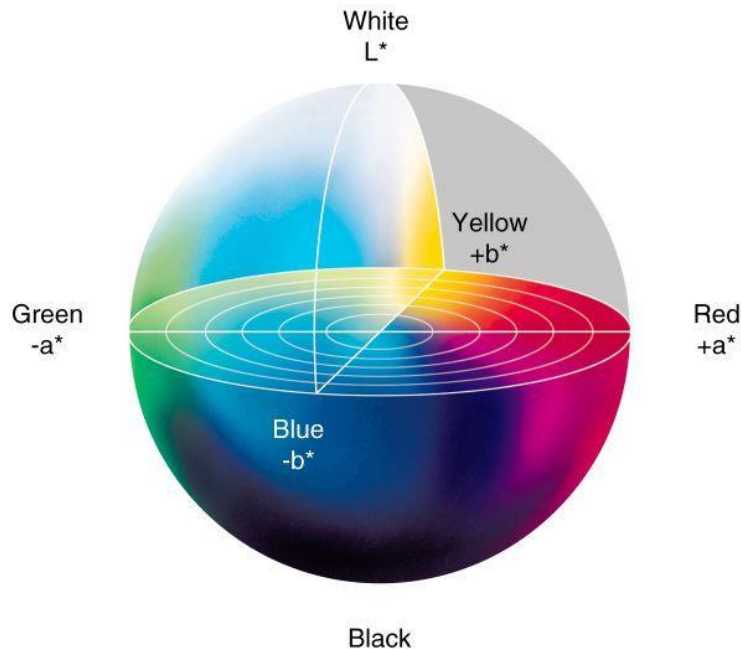


Figure 2.3: $L^* a^* b^*$ color model [36].



(a)



(b)

Figure 2.4: A sample image in (a) RGB color space, (b) $L^*a^*b^*$ color space.

2.2.3. HSV Color Space

The HSV color space attempts to characterize colors according to their hue, saturation, and value (brightness) shown in Figure 2.5.

This color space is based on a so-called hex-cone model which can be visualized as a prism with a hexagon on one end that tapers down to a single point at the other. The hexagonal face of the prism is derived by looking at the RGB cube centered on its white corner. A sample image in $L^*a^*b^*$ and RGB color spaces are shown in Figure 2.6.

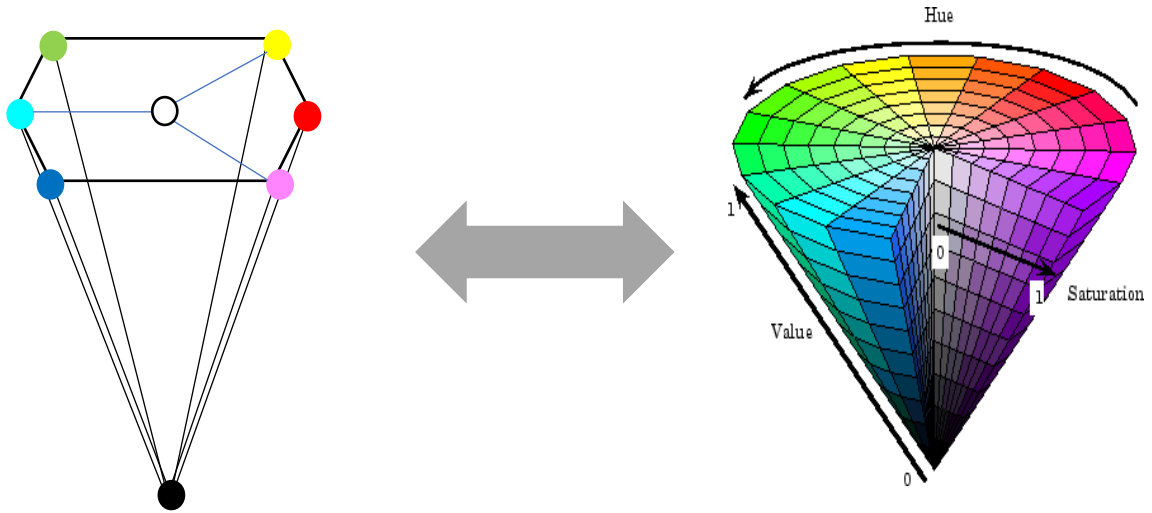


Figure 2.5: HSV color model



(a)



(b)

Figure 2.6: A sample image in (a) RGB color space, (b) HSV color space

In general, image, retrieval can be done depending on several features, mainly, color, texture, and shape of the target image contents. Those techniques which are dependent on the texture and shape of the image contents are among spatial information-dependent methods. On the other hand, a color histogram does not depend on spatial information of image content.

2.3. Image histogram matching techniques

A color histogram is a vector representing the distribution of colors in an image. In digital imaging, histograms are graphs representing the number of pixels in an image, usually in the RGB color space. Images are set to have the same number of pixels before taking the histogram. Due to the simple computation and also exhibit attractive properties, color histograms are the most frequently used in image retrieval [37], [38], [39]. Color histograms do not carry information about the spatial features of given color pixels. Moreover, color histograms are resistant to modification in camera viewpoint. Since the only information which is stored in a color histogram is color, images with identical histograms can appear distinct [40], [41].

Conventional Histogram Intersection (HI), Merged Palette Histogram Matching (MPHM) and Gaussian Weighted Histogram Intersection (GWHI) Methods are three popular histogram-based image matching techniques which all are briefly discussed next.

2.3.1. Conventional Histogram Intersection (HI) Method

Histogram-based image matching algorithms try to measure the resemblance of image contents by their color histograms between a query image and images from the data set (reference images), to categorize or retrieve images. Histogram intersection (HI), proposed by Swain and Ballard [42], [43], is a direct and simple technique to compute the matching level between two color histograms.

Suppose, the color histograms of a query image and the color histogram of a reference image are HM and HR respectively, which each of them has n bins. Intersection HI of two histograms is defined in [43] as:

$$HI = \sum_{i=1}^n \min (h_M(i), (h_R(i))) \quad \text{Eq.4}$$

The subscripts “ M ” and “ R ” shows the “model” and “Reference” respectively. The values for both HM and HR are normalized as:

$$\sum_{i=1}^n h_M(i) = 1, \quad \sum_{i=1}^n h_R(i) = 1 \quad \text{Eq.5}$$

The consequent fractional matching value between 0 and 1 is the proportion of pixels from the query image that have corresponding pixels of the same color in the reference image. A higher histogram matching level illustrates a greater resemblance between the query image and the reference image.

2.3.1.1. Limitations of Conventional HI Algorithms

The conventional HI algorithm has an important limitation to compare different histograms. This method considers identical color matching, so corresponding pixels of identical colors can be compared and matched. Though, practically the colors in real images can be distorted both in the scene itself and in the image capturing process. Therefore, using HI algorithm will decay the similarity level significantly for images where their visual information is the same, but still, there is slight color variation.

In

Figure 2.7, three “pink” images are taken as an example to illustrate this problem. Three images are similar to each other, however the “Query image 1” is more similar to “Reference image” than “Query image 2”. The reference image is a monotone color image where all pixels are $(R,G,B) = (210,90,124)$. The difference between two histograms are taken by absolute difference between the reference image the query image. It is seen that the “Reference image” is more similar to “Query image 1” rather than “Query Image 2”. However, the conventional histogram matching method gave the same amount of difference for the comparison between reference image and the two query images.

2.3.2. Merged Palette Histogram Matching (MPHM) Method

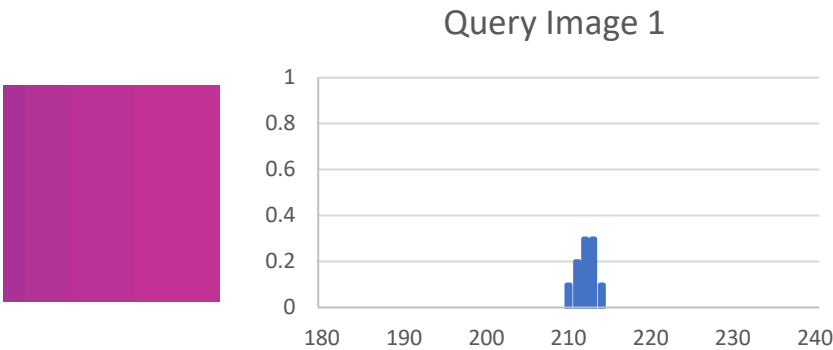
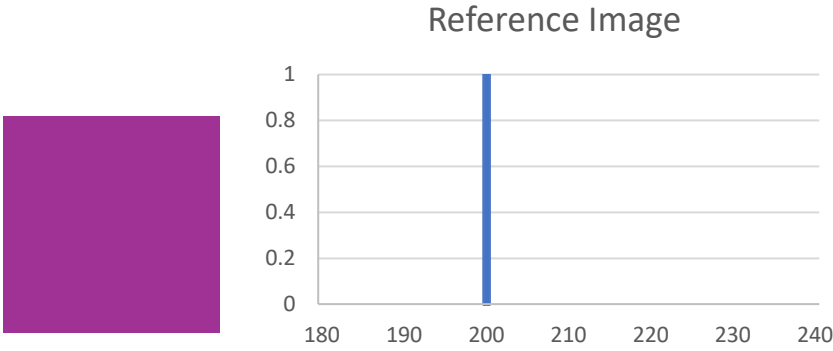
The conventional HI algorithm provides a straightforward and robust method to measure the similarity between two images. By such a way, the image matching problem is converted to a simple problem that, to what extent the histogram of the query image is similar to that of the reference image. However, as it stated section 2.3.1.1, this algorithm has a limitation which only works on corresponding pixels of identical colors.

To solve this problem, Wong and Cheung [44] introduced a merged palette histogram matching (MPHM) technique. The scope of their method is to expand the intersection from pixels of identical colors to pixels of similar colors. The intersection between the pixels of the two colors can be achieved, in case the distance between two colors is less than a given threshold.

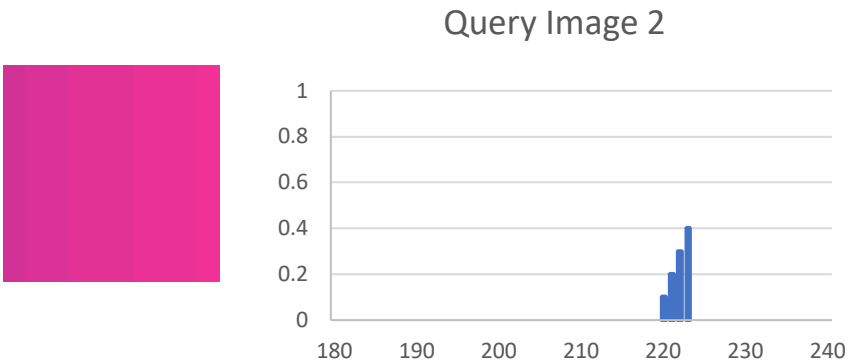
2.3.3. Modified Color Histogram Method

Similar to (MPHM), Modified color histogram matching technique provides a solution for the limitation stated in section 2.3.1.1 for monotone color images' classification. This method helps in extending the similarity and give specific weight to those histograms which are more similar to the reference image.

To have a valid comparison, a Gaussian distribution should be assigned for the monotone color histogram, as shown in **Figure 2.10**. The Gaussian distribution is defined with a mean of values for R, G, and B of the monotone color histogram. So, it can be easily concluded that "Query Image 2" is the most similar sample to our reference image. The same example shown in Figure 2.7 is again repeated by replacing the single bar histogram with a Gaussian distribution. The result for this example is demonstrated in Figure 2.8. Using the Modified Histogram matching method helped to identify the difference between two images. The result for absolute difference between the "Reference image" and "Query image 1" is equal to 1.8, whereas the result for absolute difference between the "Reference image" and "Query image 2" is equal to 1.95. Lower amount of difference shows a higher rate of similarity. Therefore, it is concluded that "Query image 1" is more similar to "Query image 2".



$$\sum_{i=1}^N |R_i - Q_i| = 2$$



$$\sum_{i=1}^N |R_i - Q_i| = 2$$

Figure 2.7: An example for the problem with the conventional HI algorithm

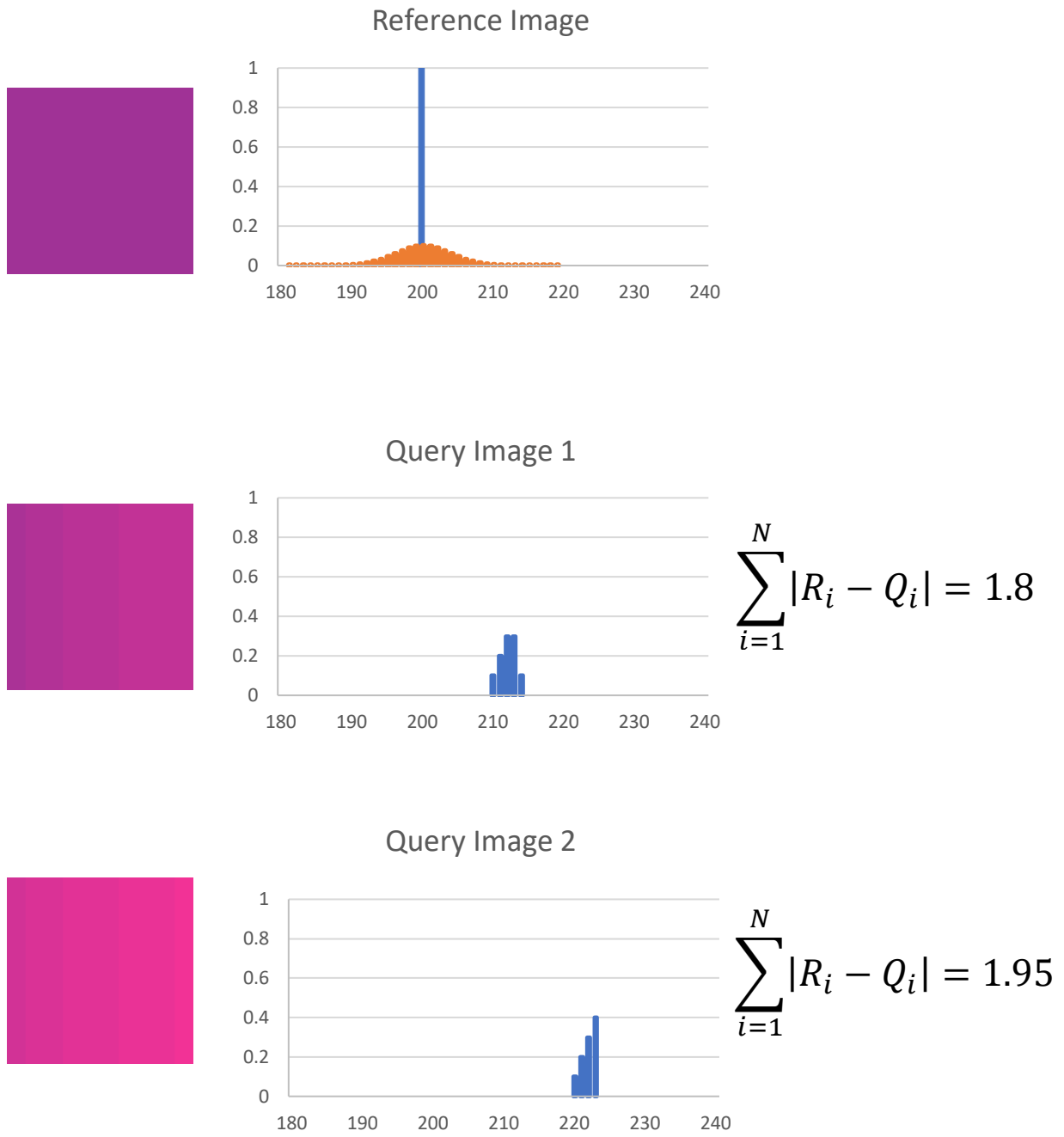


Figure 2.8: The solution for the problem with the conventional HI algorithm, using Modified Histogram matching method

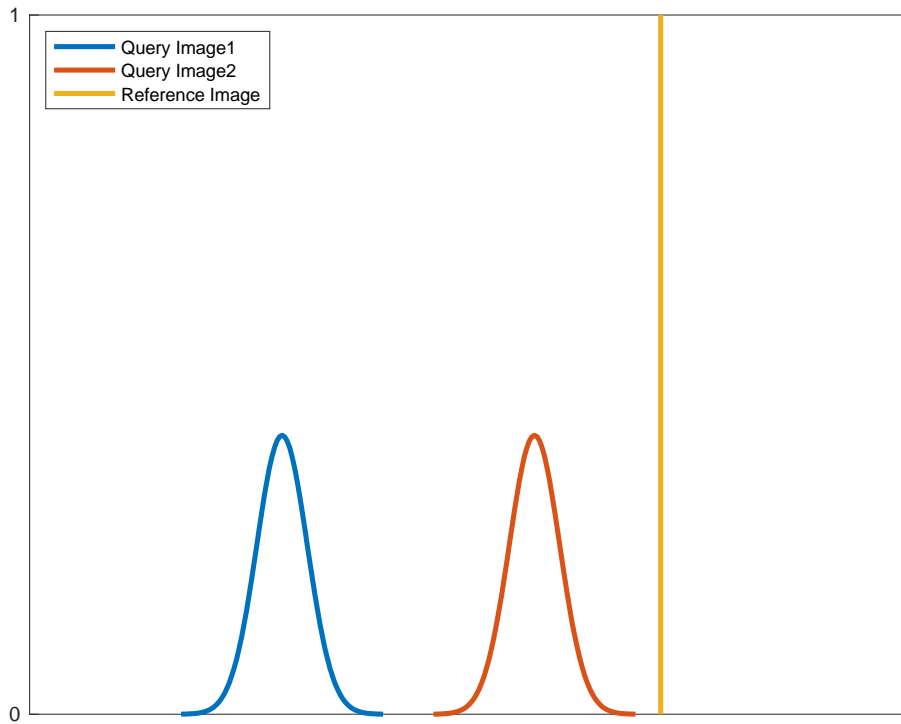


Figure 2.9: Two Query images histogram compared to a sample reference image

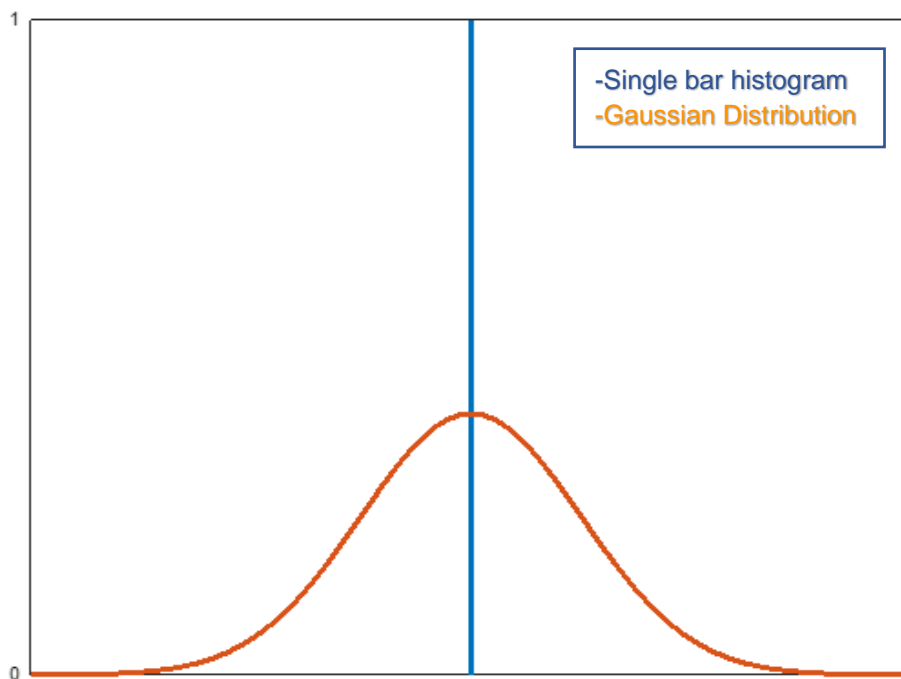


Figure 2.10. Modified single bar histogram using Gaussian distribution

2.4. Distance measurements technique

A central problem in image recognition and computer vision is determining the distance between images. Many efforts have been made to define image distances which provide intuitively reasonable results. In image analysis, a distance transform measures the distance of each object point from the nearest boundary [45]. In this section, commonly used distance measurement methods have been introduced briefly.

The Euclidean distance is the straight-line distance between two pixels and is evaluated using the Euclidean norm. The city block distance metric measures the path between the pixels based on a four connected neighborhood and pixels whose edges touch are one unit apart and pixels diagonally touching are two units apart. The chessboard distance metric measures the path between the pixels based on an eight connected neighborhood. The quasi-Euclidean metric measures the total Euclidean distance along with a set of horizontal, vertical, and diagonal line segments.

2.4.1. Euclidean distance

The Euclidean distance is the distance between two points in Euclidean space. Euclidean distance algorithm computes the minimum distance between a column vector x and a collection of column vectors in the codebook (CB) matrix. A codebook is a type of document used for gathering and storing codes. Originally codebooks were often literally books, but today codebook is a byword for the complete record of a series of codes, regardless of physical format.

In one dimension, the distance between two points, x_1 and x_2 , on a line is simply the absolute value of the difference between the two points as Eq.6.

$$\sqrt{(X_2 - X_1)^2} = |X_2 - X_1| \quad \text{Eq.6}$$

In Euclidean space, the distance between two points, p , and q is defined as the square root of the sum of the squares of the differences between the corresponding coordinates of the points (Eq.7). Among all the image metrics, Euclidean distance is the most commonly used due to its simplicity.

$$d(a, b) = \sqrt{(p_1 - q_1)^2 + (p_2 - q_2)^2} \quad \text{Eq.7}$$

Due to the simplicity and being straight-forward, Euclidean distance is selected as a spatial dependent method to calculate the distance between a query image and a set of reference images.

2.4.2. City Block Distance

Another popular measure is the Manhattan (or city block) distance, named so because it measures the distance in blocks between two points in an image. The value for the city block distance is always greater than or equal to zero. The measurement would be zero for identical points and high for points that show little similarity. The city- block distance measuring horizontal and vertical directions.

The city block distance transform is a basic operation in computer vision, pattern recognition, and robotics. For instance, if the black pixels represent the target points, then d_{ij} tells us how far the point (i, j) is from these target points.

$$d_{ij} = \sum_{k=1}^n |x_{ik} - x_{ij}|; \quad \text{Eq.8}$$

2.4.3. Chess Board Distance

The chessboard distance is a metric defined on a vector space where the distance between two vectors is the greatest of their differences along any coordinate dimension. In two dimensions, if the points P and Q have Cartesian coordinates (x_1, y_1) and (x_2, y_2) their chessboard distance is defined as:

$$D_{Chess} = \max (|X_2 - X_1|, |Y_2 - Y_1|) \quad \text{Eq.9}$$

Danielsson (1980) asserted that both Manhattan and chessboard distance are rarely used [46].

2.5. Validation Set

Applying the proposed algorithms on a validation set helps to assess the success rate of the chosen methods. This validation set is created by applying a perturbation on pre-defined reference images. Precisely, Generalized Extreme Value Distribution (GEVD) method is utilized to make a skewness shape on histogram of the monotone color reference images. A simple comparison between the known perturbed validation set and the original reference images will provide the success rate for each of the applied algorithms.

2.5.1. Generalized extreme value distribution

Generalized Extreme Value Distribution (GEVD) provides a limiting distributions for maxima or minima (extreme values) of an identically independent random variable. Using the standardized variable which is the location parameter and is the scale parameter, the Probability Distribution Function (PDF) of the extreme value distribution is described as below [47]:

$$\frac{1}{\sigma} t(x)^{\xi+1} e^{-t(x)} \quad \text{Eq.10}$$

Where:

$$t(x) = \begin{cases} \left(1 + \xi \left(\frac{x - \mu}{\sigma}\right)\right)^{-1/\xi} & \text{if } \xi \neq 0 \\ e^{-(x-\mu)/\sigma} & \text{if } \xi = 0 \end{cases} \quad \text{Eq.11}$$

ξ and μ are constant numbers.

Probability Distribution Function of GEVD is shown in Figure 2.11.

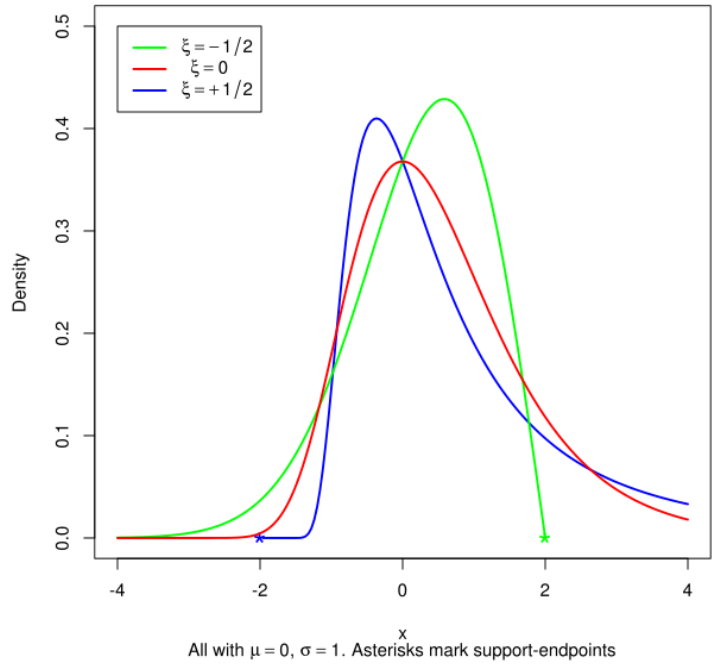


Figure 2.11: PDF of the extreme value distribution

Figure 2.11 shows a skewness for GEVD on whether left or right side. The reason for using this distribution is to create a perturbation to evaluate our algorithm's limitations. The skewness in GEVD will cause an overlap between the reference image histogram and also the query image histogram. This will show the most similar reference image as the result for image retrieval. Applying this, also, will help us to examine how accurate our algorithm can act by increasing the amount of skewness in distribution of the reference image set. This parameter should be set in a way that it covers only one reference image histogram, otherwise there might be more than one result for the image retrieval. Consequently, we can achieve a success rate for each of our proposed algorithms. The results of the validation set application in chosen algorithms are demonstrated in chapter 3.

Chapter 3. Experimental Results for Skin Color Classification

3.1. Introduction

In this chapter, the methods studied in chapter 2 are applied on two sets of pre-defined reference sets to retrieve a query image from a set of reference images. The first method is the Euclidean distance studied in section 2.4.1. This spatial dependent algorithm compares the input image with a pre-defined set of reference images in RGB color space.

The second method uses the color histograms of query images and the pre-defined reference images. The histograms are then compared to measure the similarity between two sets of images the query image.

The proposed algorithms have been implemented on two types of reference skin images. Each group of reference images shows different skin tone categories, which includes skin tones starting from light colors to darker tones.

The first category of skin color reference images is created based on the Fitzpatrick Skin scale color codes. Fitzpatrick color codes have been provided in Table 3.1 [48]. The reason for selection of this scale among other introduced scales is the availability of the color codes. These color codes gave us the possibility of creating an exact color of the Fitzpatrick scale. Though, the other color scales which have been stated in chapter 1 do not have any reference color codes. The Second category was driven from a well-known cosmetic brand, Dior [24], which uses a skin tone palette with more colors of skin shades. This category comprises twelve colors of skin.

In order to confirm the accuracy of our algorithms, two different sets of query images have been tested on proposed algorithms. The first set of query images have been reproduced from the original reference sets. This new set of query images have been created by applying a perturbation on the reference images using “Extreme Value Distribution” method. The second set of query images are from an online website which aims to collect different types of human skin races [30]. Different parts of the images such as face, neck, and shoulder are cropped from the portrait images to provide the required query images.

All studies for image retrieval were conducted using RGB color space. HSV color space and $L^*a^*b^*$ color space have also been tested on our algorithms, however, due to the low accuracy of these color spaces for monotone color images, RGB color space has been chosen as a proper color space to apply on our algorithms.

Table 3.1: Fitzpatrick Color Codes

Color Type		Color Code
Class 1	Pale White	U+1F3FA
Class 2	White	U+1F3FB
Class 3	Cream White	U+1F3FC
Class 4	Moderate Brown	U+1F3FD
Class 5	Dark Brown	U+1F3FE
Class 6	Black	U+1F3FF

3.2. Validation Set Generation Using Extreme Value Distribution

The Generalized Extreme Value Distribution was introduced in chapter 2, section 2.3. This method is used to create a set of perturbed query images from original reference images. These set of query images are used as the validation set for the proposed algorithms. The validation sets for both pre-defined data sets (Fitzpatrick scale and Dior skin color palette) are presented in this chapter. Both validation sets are tested in proposed algorithms, and the success rate is established separately for each algorithm.

To be more accurate, the RGB values of the data set images are read by using the latest release of Photoshop software [49]. Next, the images are created based on their RGB values for further studies.

Common methods for image generation from a set of RGB histogram have the main drawback, which can highly impact the accuracy of the output images. The color histogram provides the information about the available color distribution of the given image, regardless of the information about location of each color pixel. The image creation based on RGB information gives a series of random images which includes skin-nonrelated color spectra in pixel size. This

feature has highly affected the quality of our implemented algorithms since the reference image sets are all made by their RGB information. In section 3.2.1, this obstacle is comprehensively introduced, including our proposed solution.

3.2.1. Organized Image Creation Using RGB Color Histograms

Images are created by using RGB color histograms information. A monotone color image can be generated by applying a combination of RGB values, which are randomly picked from color histograms. The order of selecting RGB values from color histograms is of utmost importance, because a random selection of RGB color values may provide some results which are not useful for a specific application. Below is an example which clearly illustrates the problem for the random selection of RGB values.

Let us consider nine different points on RGB histograms separately. There are three points in Red color histogram as: (R_1, R_2, R_3) . Similarly, there are three points in Green and Blue color histograms as well: (G_1, G_2, G_3) and (B_1, B_2, B_3) . Considering these values, there will be 84 possible colors which can be produced by these nine values in the RGB histogram. Most of these colors contain pixels with various colors which are not in skin shades. A well-formed solution has been introduced to address this problem.

A normal distribution with a mean value of zero and variance of 10 is defined ($\mu = 0, \sigma = 10$). The random values for this distribution can be assumed as $\{x_1, x_2, x_3, \dots, x_n\}$.

In order to create color images with similar shades of skin colors, the mean value of reference color histograms will be sum up by the random values of generated normal distribution. Consequently, the new RGB histograms for point one will be as:

$$R_{New} = (R_1, R_1 + x_1, R_1 + x_2, R_1 + x_3, \dots, R_1 - x_n)$$

$$G_{New} = (G_1, G_1 + x_1, G_1 + x_2, G_1 + x_3, \dots, G_1 - x_n)$$

$$B_{New} = (B_1, B_1 + x_1, B_1 + x_2, B_1 + x_3, \dots, B_1 - x_n)$$

The new set of values for RGB colors are ready to create monotone color images which all are in shade of the skin color.

3.2.2. Application of GEVD on Fitzpatrick scale

The GEVD has been applied to our first set of reference images which contains Fitzpatrick skin monotone color images. Results have been demonstrated in Figure 3.1 and Figure 3.3. The color histograms for the Fitzpatrick scale images are demonstrated in Figure 3.2.

Based on what previously stated in part 2.3, GEVD technique has minimum and maximum extreme values, which limits the sample sizes. A minimum value of $\sigma - 10$ and a maximum value of $\sigma + 30$ has been applied on our distribution. Applying extreme values on image histograms should not impact the number of the pixels of the histogram. Therefore, the number of the pixels which are cut before $\sigma - 10$ and also after $\sigma + 30$, will be added to a number of pixels on the mean value.

3.2.3. Application of GEVD on Dior Skin Color Palette

In this section, GEVD has been applied to a skin color palette from Dior cosmetic products. The color histograms for the Dior skin palette are presented in Figure 3.5. The perturbed results for this set of reference images are shown in Figure 3.4 and Figure 3.6. Similar to Fitzpatrick reference validation set, GEVD has been created separately around each of the (R, G, B) color histograms with a skewness to the left side. The minimum value of $\sigma - 10$ and a maximum value of $\sigma + 30$ has also been applied on Dior skin color palette distribution. Also, number of removed pixels by extreme minimum and maximum limitations are already added to the number of pixels on mean value.

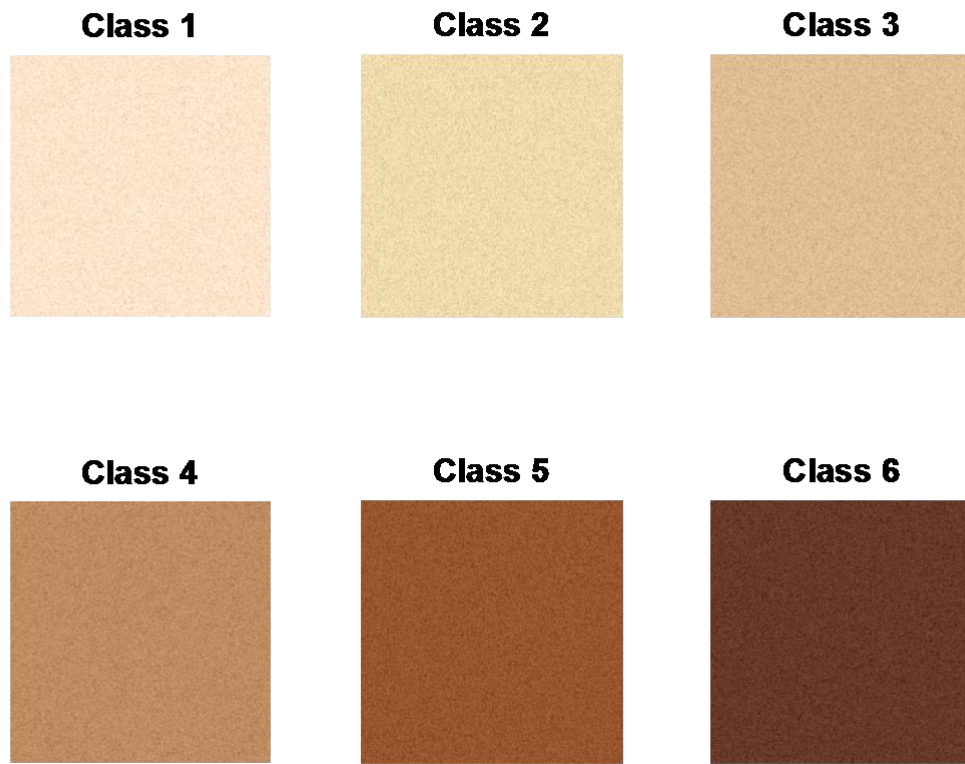


Figure 3.1: Perturbed Fitzpatrick scale

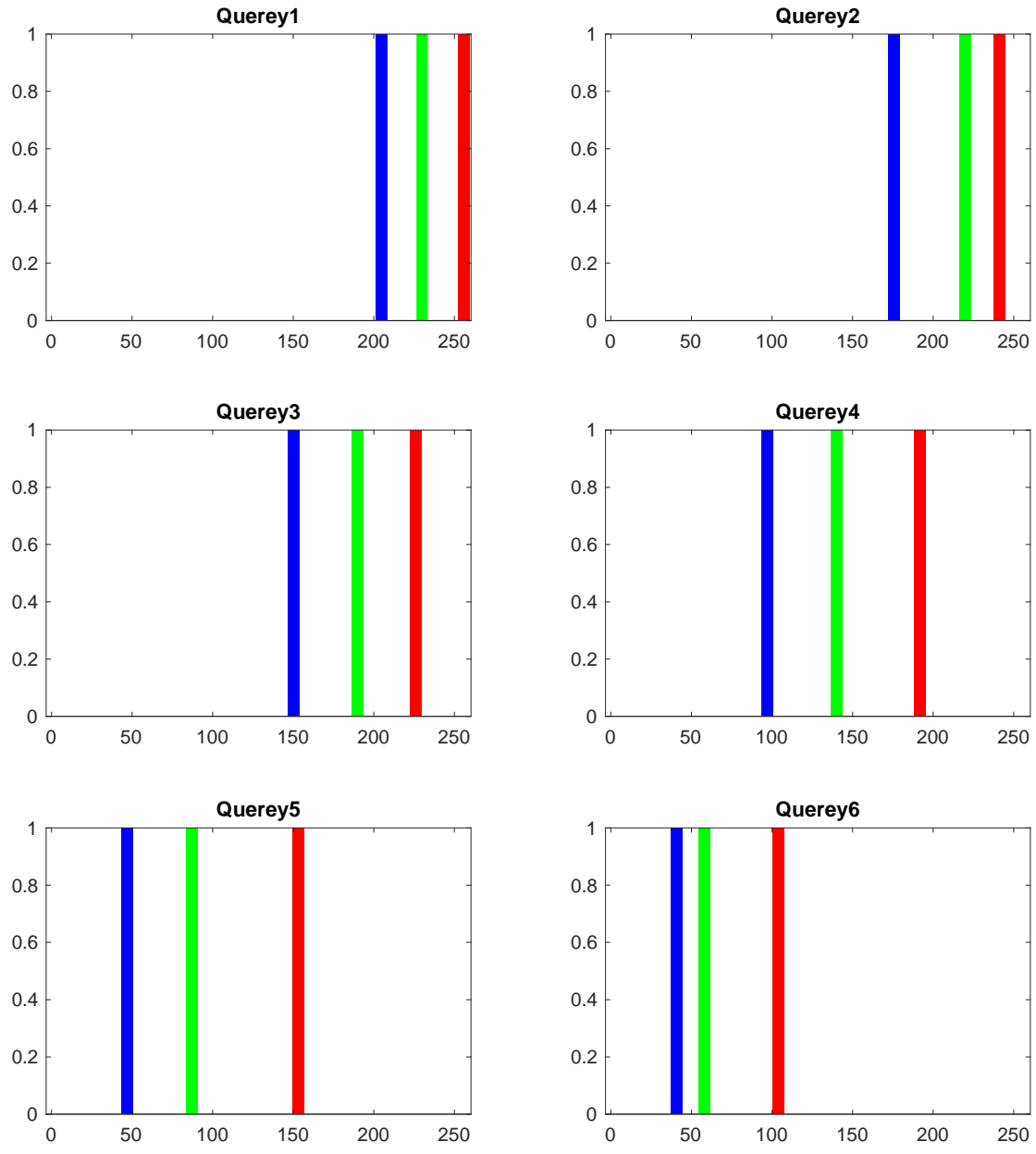


Figure 3.2: Color histograms for the Fitzpatrick scale reference

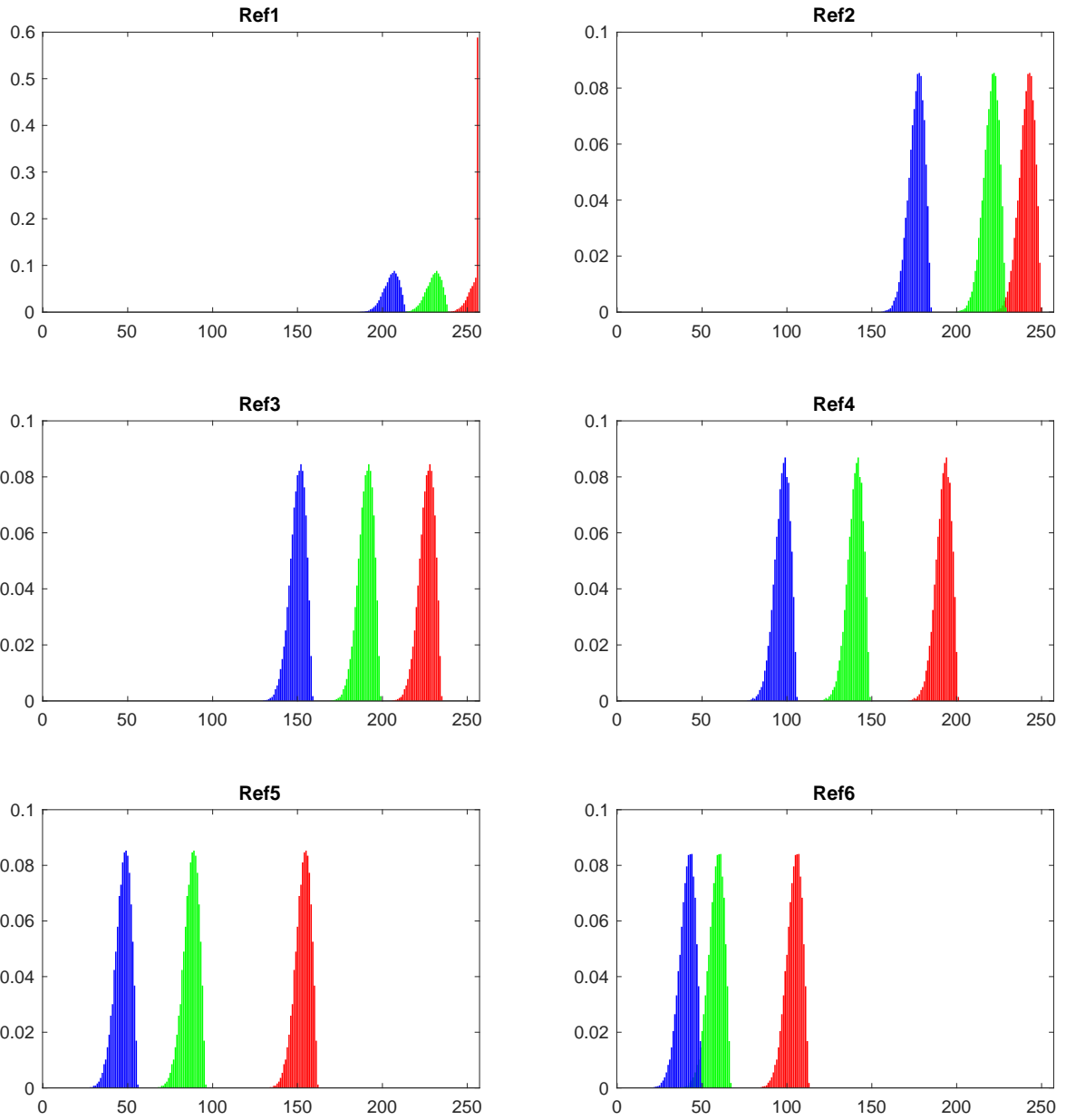


Figure 3.3: Perturbed reference image histograms for the Fitzpatrick scale.

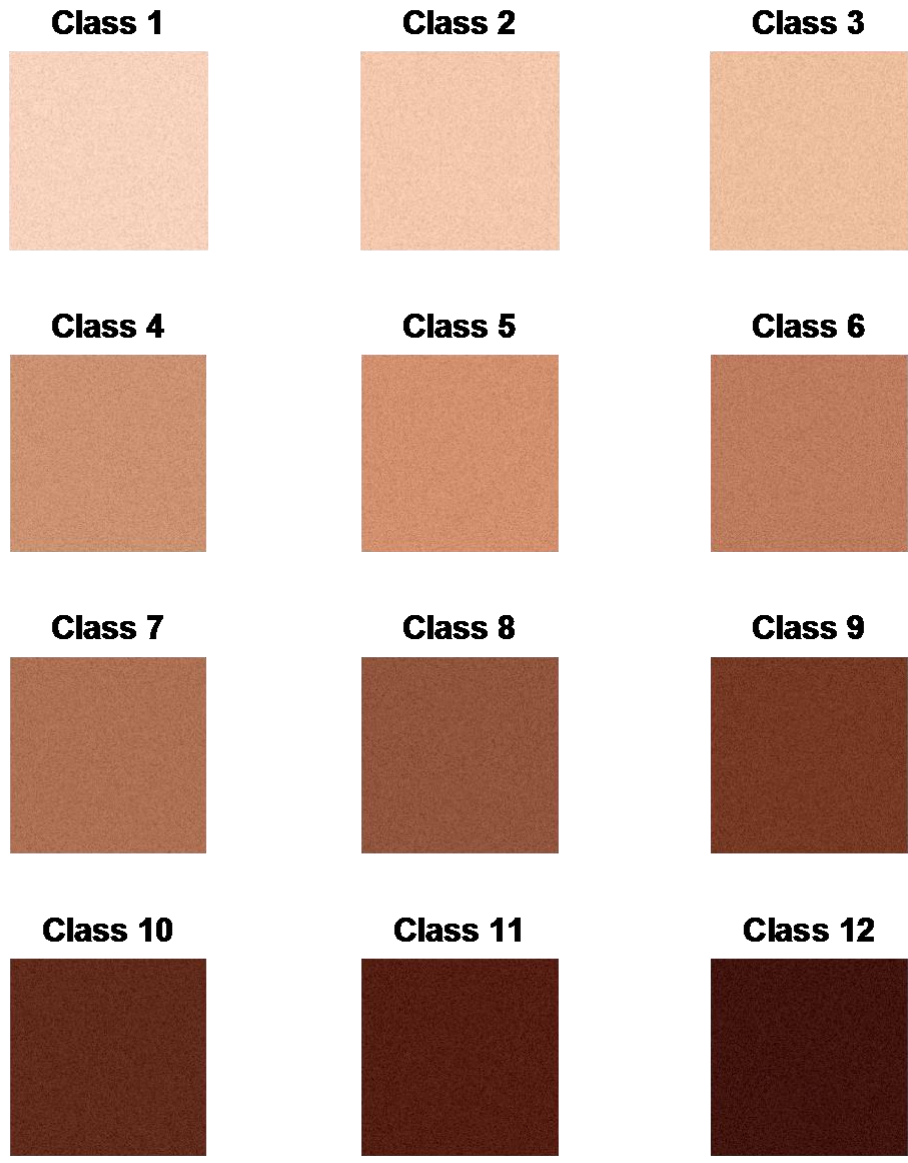


Figure 3.4: Perturbed Dior skin palette

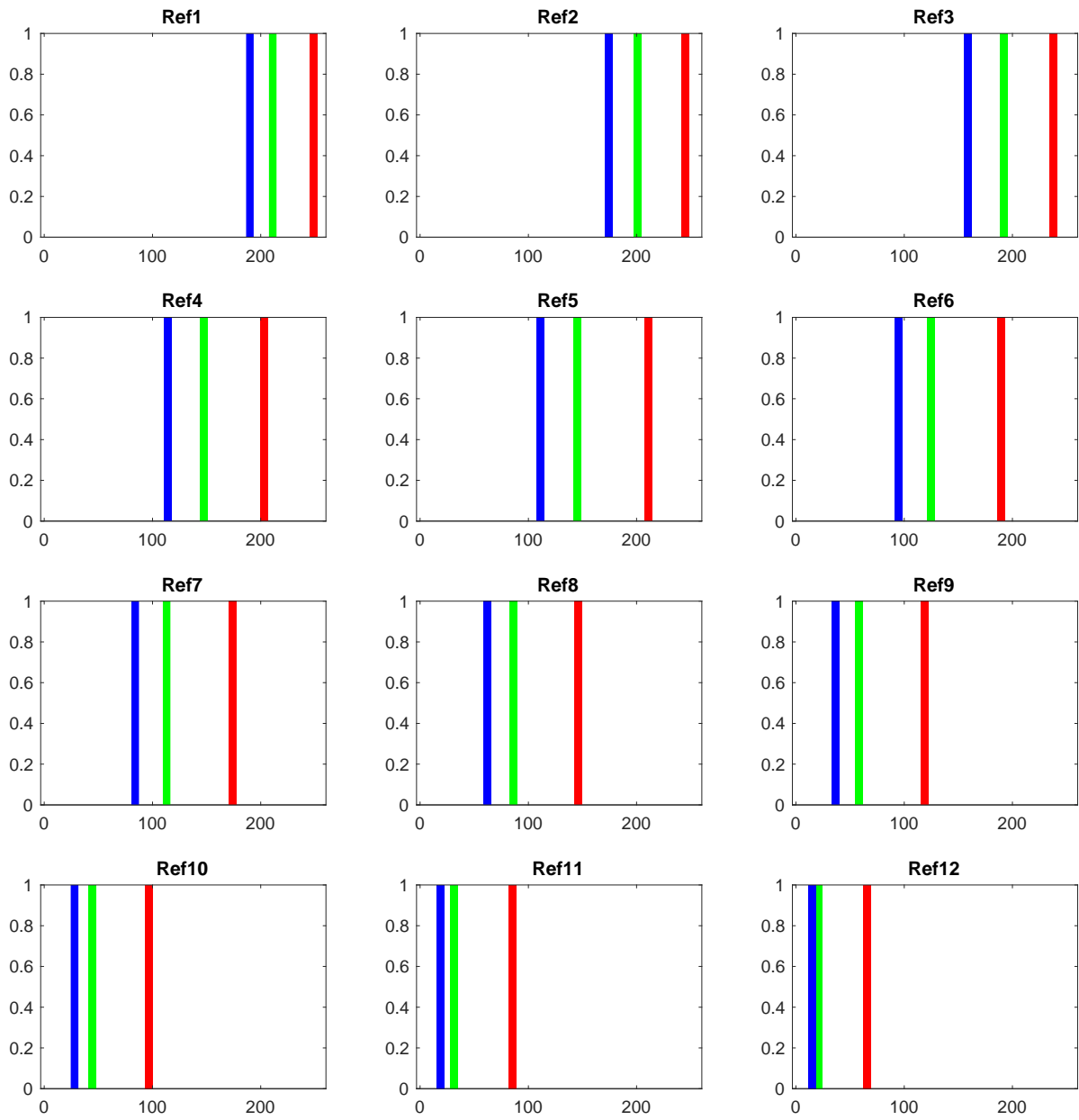


Figure 3.5: Color histograms for Dior cosmetic palette reference images

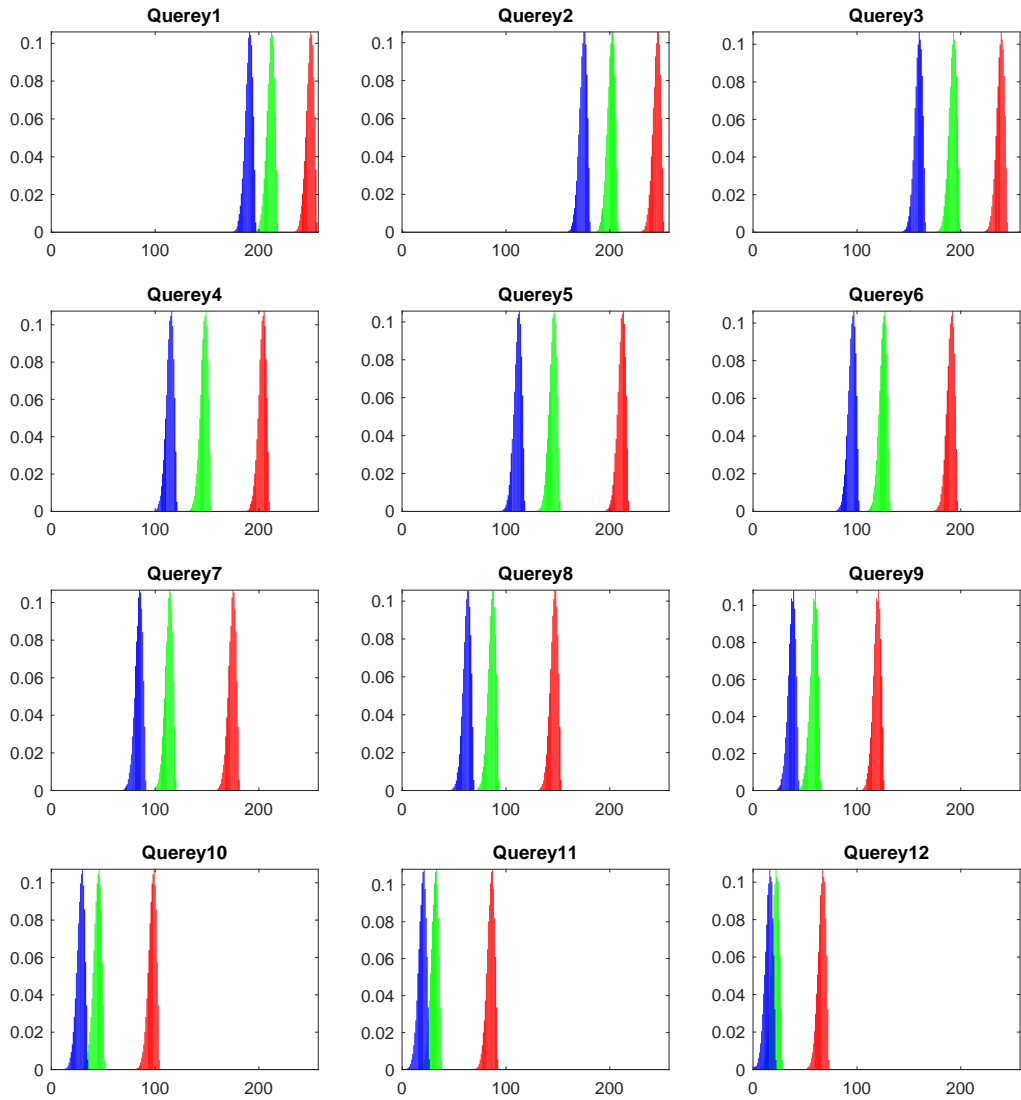


Figure 3.6: Perturbed reference image histograms for Dior skin palette

3.3. Euclidean Distance Application for Image Retrieval

As discussed in part 2.4.1, Euclidean distance between two points (p and q) is defined as the square root of the sum of the squares of the distance differences between the corresponding coordinates of the points (p, q). This method is considered as a spatial dependent technique to measure the difference between to images. In this research, “Euclidean distance” method can give us a straightforward solution for the color comparison because the images this study deals with are all monotone color.

Perturbed data sets which had been generated by applying GEVD on both the Fitzpatrick scale and also Dior cosmetic palette are used in this part of the study. The validation sets are compared with the original image reference sets by using “Euclidean Distance” method to retrieve images from the original data set.

The results are shown in

Figure 3.7 and

Figure 3.8. The horizontal axis shows each class of the Fitzpatrick scale and Dior skin palette, respectively, while, the vertical axis shows the rate of DI for both scales, respectively.

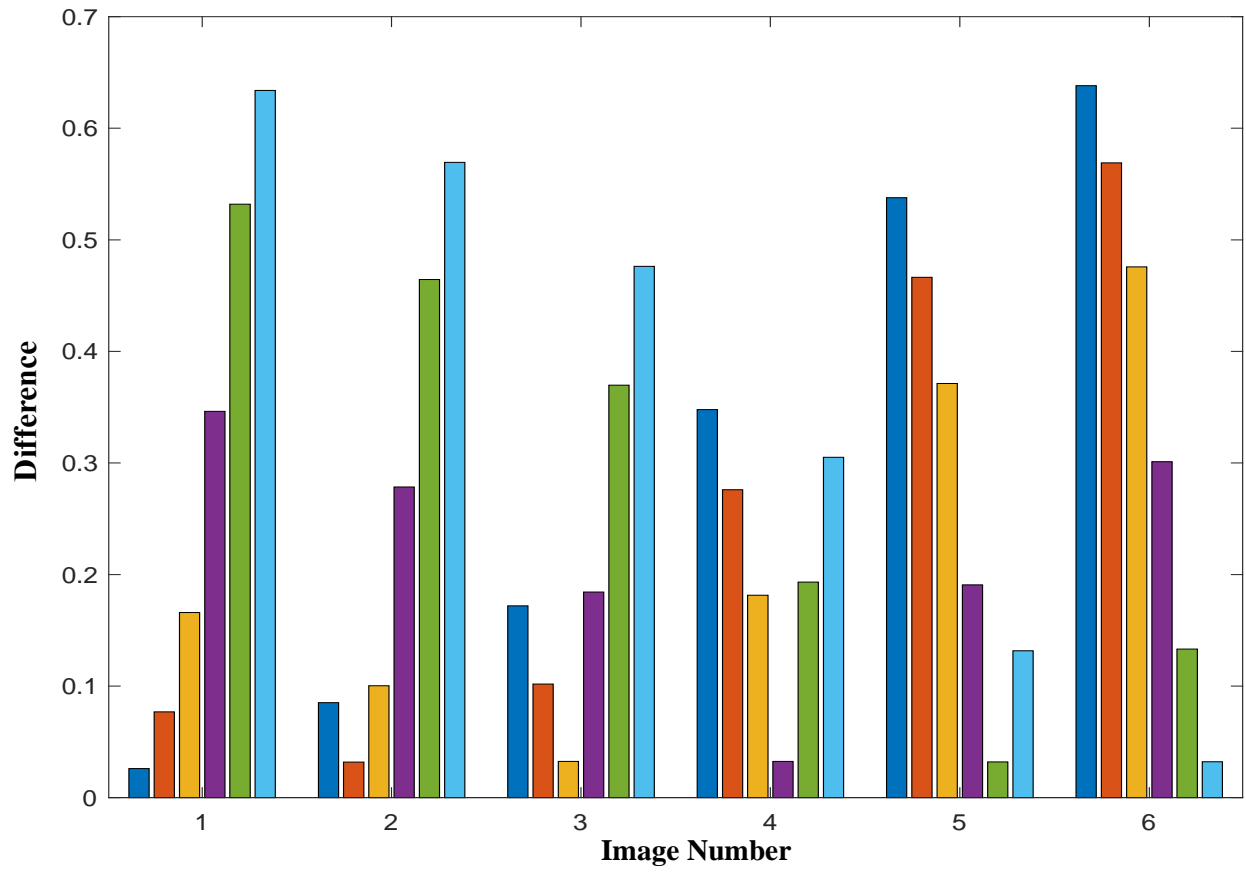


Figure 3.7. Fitzpatrick scale image retrieval, using “Euclidean distance”

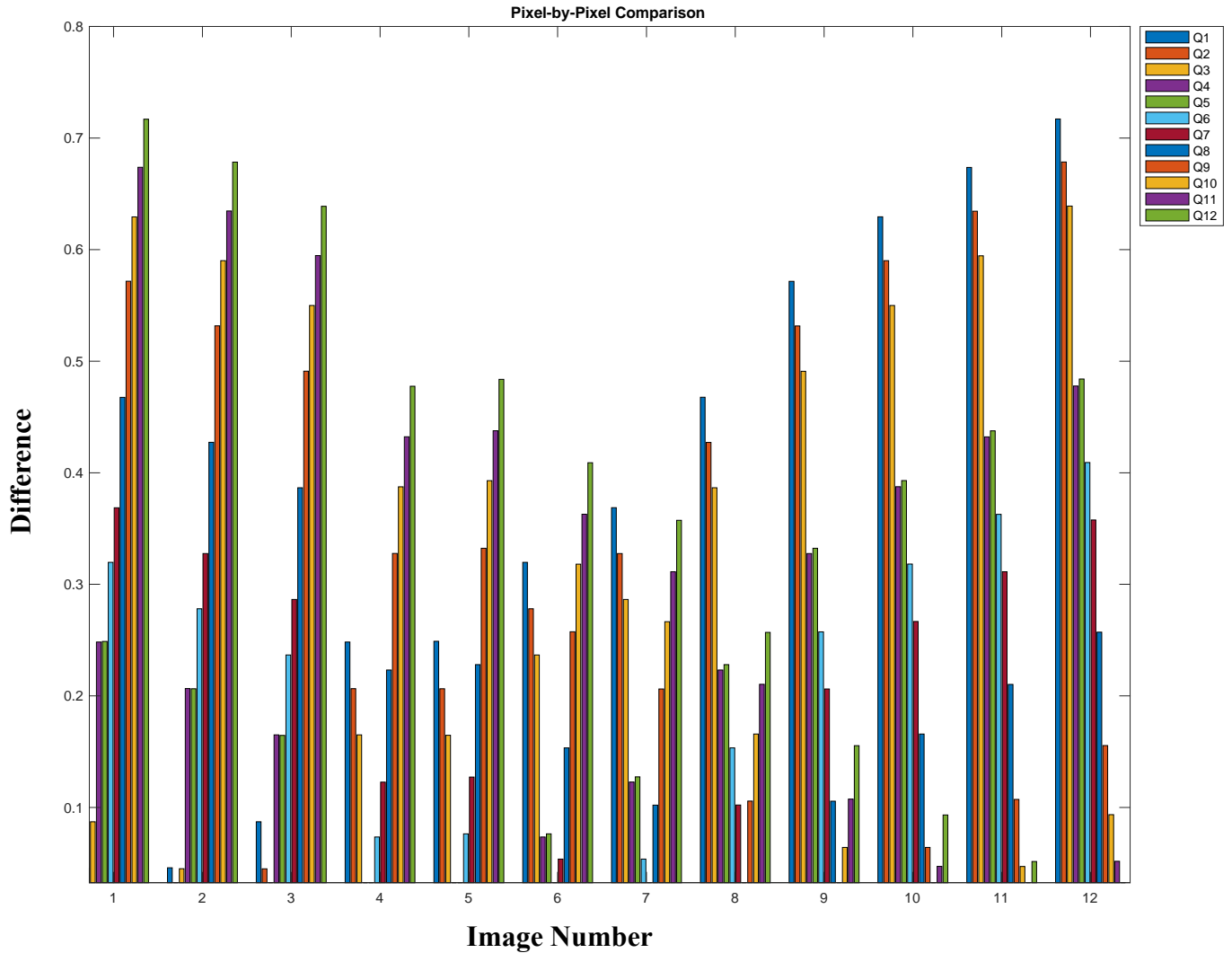


Figure 3.8. Dior cosmetic palette image retrieval using “Euclidean distance”

From the images above, it can be seen that all of the images perturbed by GEVD are perfectly retrieved in the Fitzpatrick scale and also Dior cosmetic scale. For example, image number one (shown in the blue color bar) which is the perturbed first-class reference image, is retrieved accurately in class one. The other five images are already classified correctly in their classes. At this moment, the success rate for this method will be %100.

3.4. Application of Color Histogram Matching for Image Retrieval

As stated in section 2.3, a color histogram is a vector that each input keeps the number of pixels of a specific color in the image. Histogram-based image matching algorithms try to extract the maximum similarity of image contents by their color histograms. In this section, the data set which has been extracted in sections 3.2.2 and 3.2.3 are implemented in “Modified Histogram Matching” technique.

3.4.1. The Fitzpatrick Image Retrieval Using Modified Color Histogram Matching

The color histogram for Fitzpatrick skin reference images in RGB color space is shown in Figure 3.2. The color histogram for all images is only a single bar due to the monotone color images. The size of images (number of pixels) has been normalized to deal with the small numbers (real image sizes are 200 by 200 pixel).

Figure 3.10, represents the Gaussian distribution histograms for Fitzpatrick scale reference images. As discussed in section 2.3.3, the distribution is made as a weight feature to measure the similarity around the reference images.

The amount of variance (σ) in Gaussian distribution gives the most similarity for the image retrieval. However, assigning a high variance might lead to an overlap between more than two images. As a result, the query images might be categorized in more than one classes which will provide invalid results and will decay experiments' success rate. Best on our trial and error experiments, the best value for (σ) has been set to 10 which provides the most accurate results. The experiments are done by using the perturbed query images established in section 3.2.2. Histogram matching method is done under two different cases:

- Reference images with single bar histogram.
- Reference images with Gaussian distribution histograms (Modified histogram matching method).

Results for both cases are demonstrated in

Figure 3.10 and Figure 3.11. A simple comparison of the results shows that the Gaussian distribution causes a higher ID which ends with a higher difference between images. However, single bar histogram matching method gave results with a lower ID. As the optimized result is to have a high ID, histogram matching with Gaussian distribution is a decent technique to apply on image classifications.

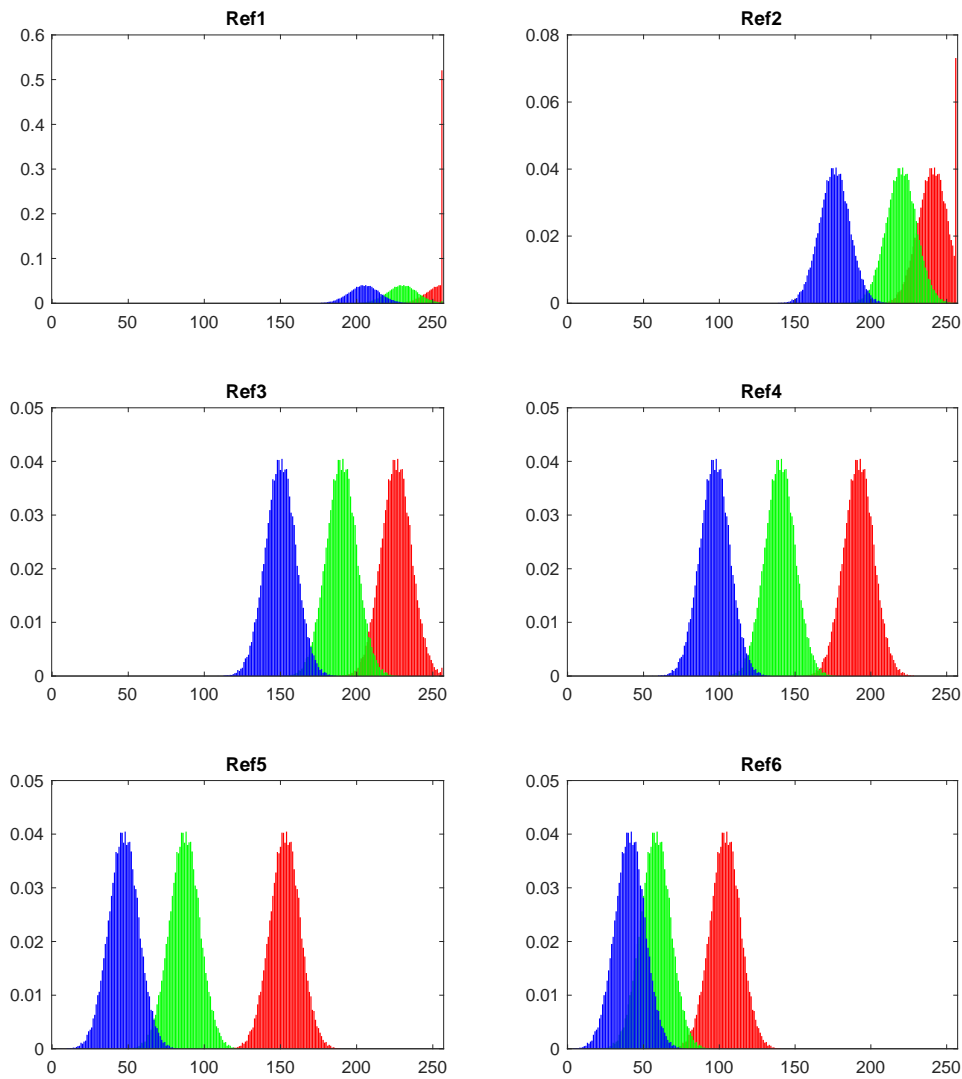


Figure 3.9. Gaussian distribution histograms for the Fitzpatrick scale reference images

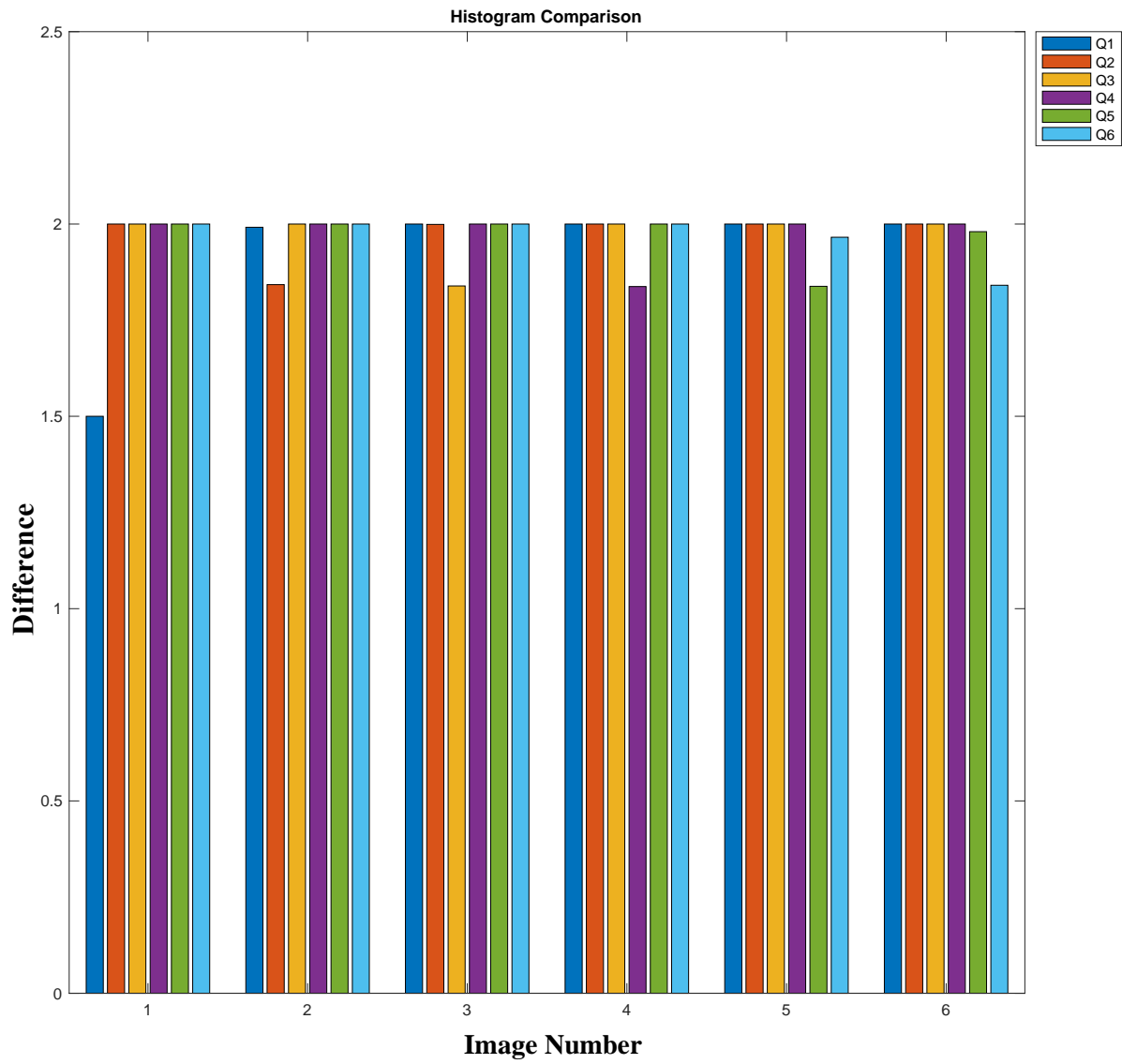


Figure 3.10. The Fitzpatrick scale image retrieval using “single bar Image Histogram”

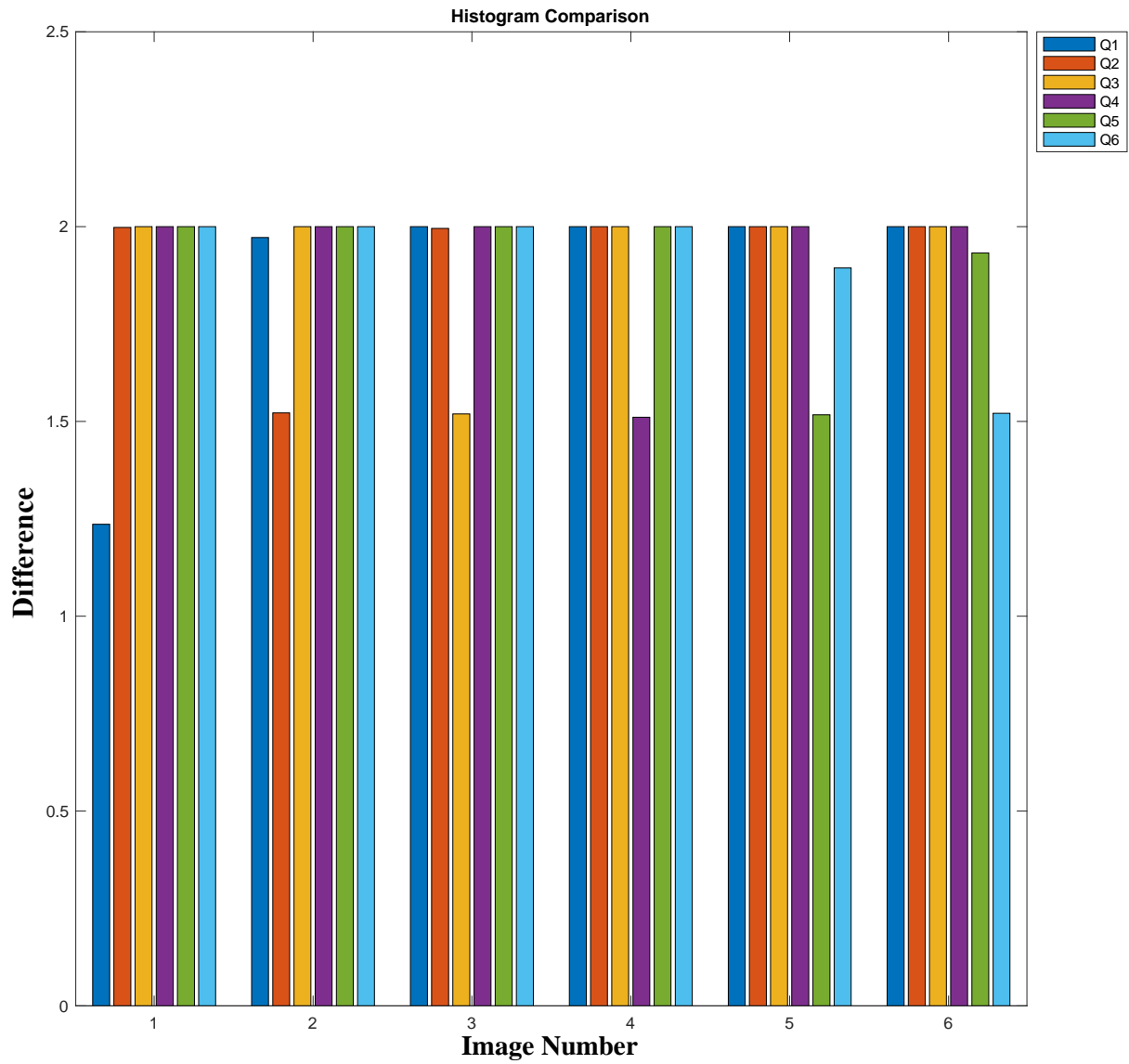


Figure 3.11. The Fitzpatrick scale image retrieval using “Modified histogram matching” method

3.4.2. Dior Palette Image Retrieval Using Modified Color Histogram Matching

In this section, image retrieval for Dior skin palette images is done by applying the Modified Histogram Matching method. The required perturbed query images (validation set) are established as discussed in section 3.2.3 and the results are shown in Figure 3.4.

Similar to the previous section, the experiments are done under two different cases:

- Reference images with single bar histogram.
- Reference images with Gaussian distribution histograms (Modified histogram matching method).

Based on the results which are presented in

Figure 3.13 and Figure 3.14, the same approach as the previous section can be concluded here as well. Modified Histogram Matching technique provided a higher ID for comparing the images. With a high ID images can be distinguished clearly and easily.

In this section, also, there is a limitation for the value of the variance in the Gaussian distribution. Similar to the previous section, this value is assigned to 10 based on trial and error experiments. Applying for this number provides the most similar and most accurate classification results.

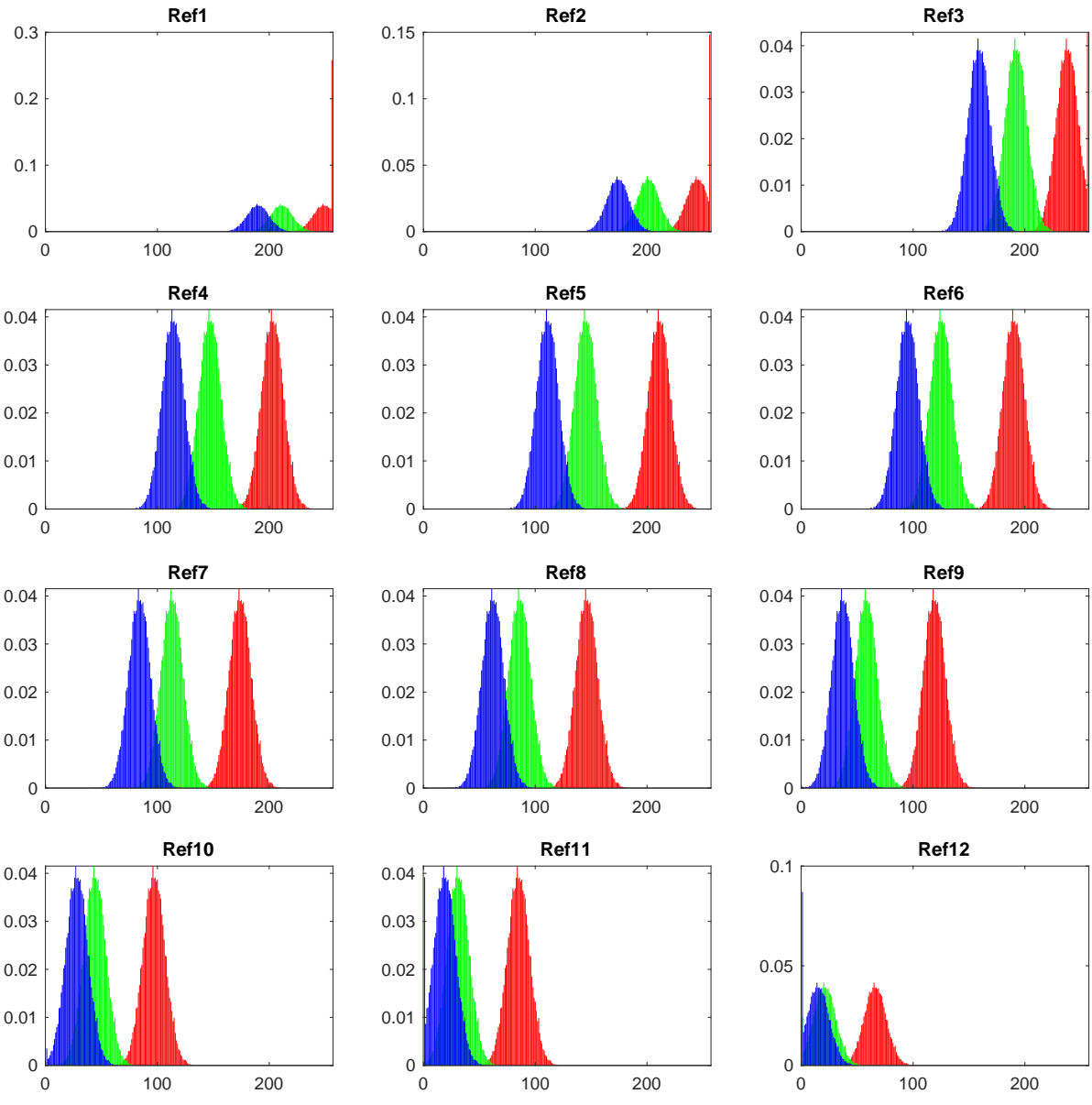


Figure 3.12. Gaussian distribution histograms for Dior cosmetic palette reference image

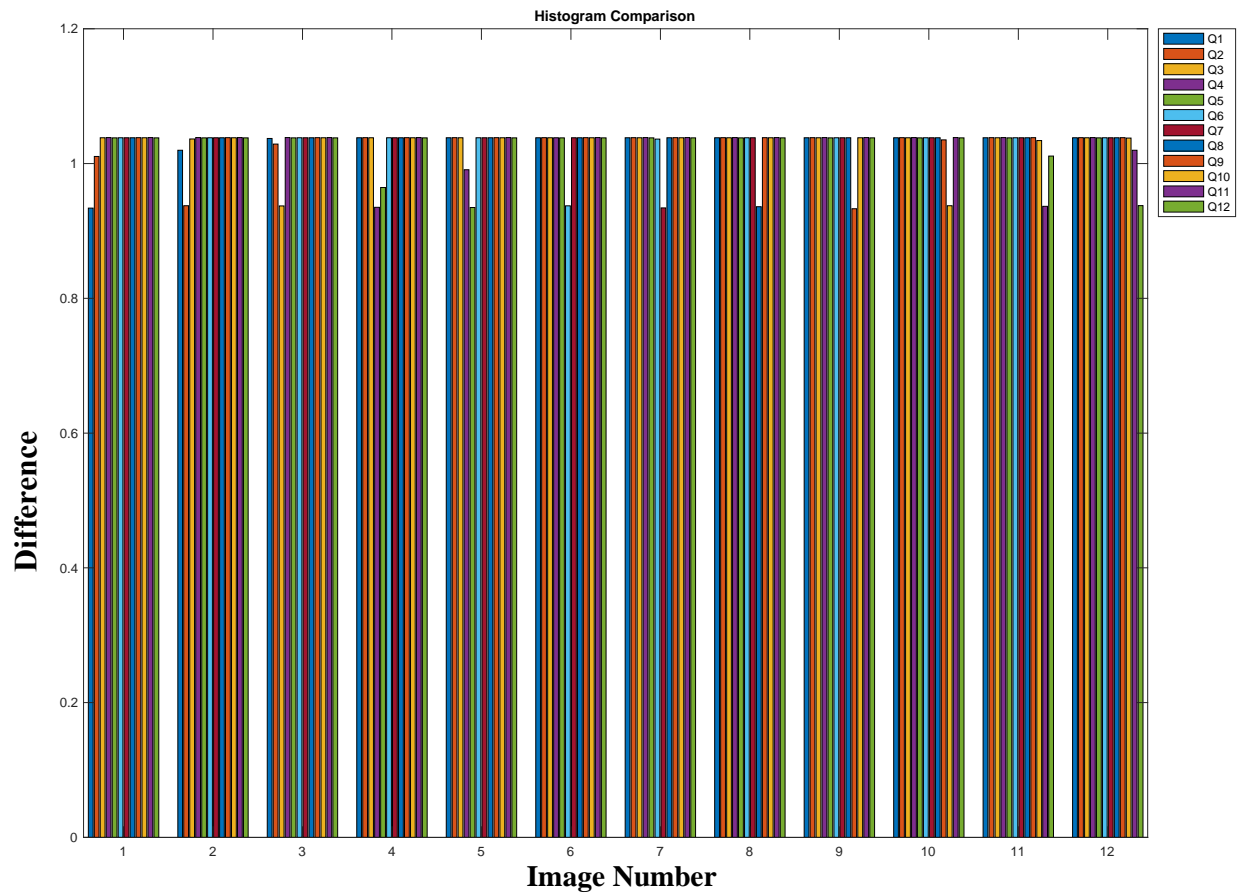


Figure 3.13. Dior cosmetic palette image retrieval using “single bar Image Histogram”

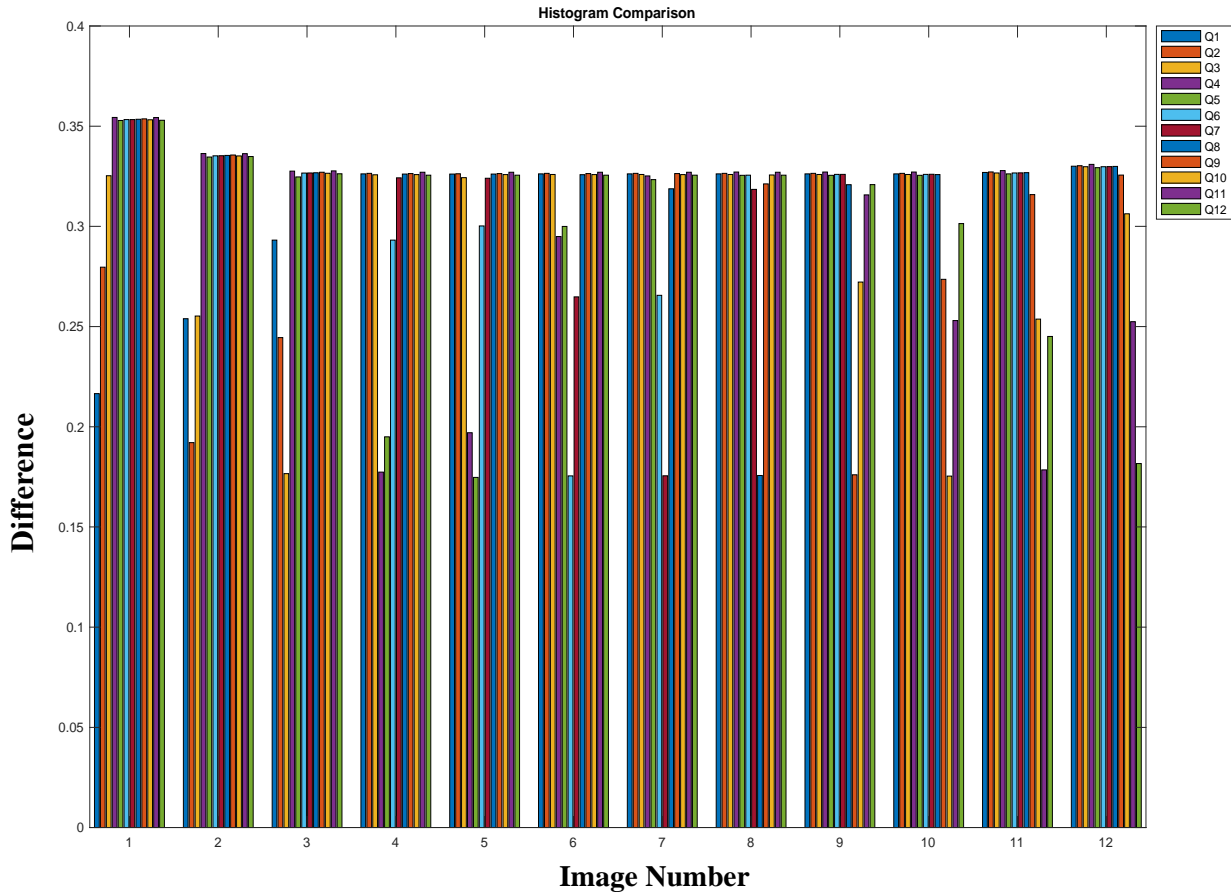


Figure 3.14. Dior cosmetic palette image retrieval using “Modified Histogram Matching.”

3.5. Application of Euclidean Distance and Modified Histogram matching methods on Real Skin Image-Set

In this section of our study, real skin images are tested by the proposed algorithms. The real skin images are provided by an online resource which aims to collect the skin tones of the entire human race based on the Pantone Color Matching System [30]. Almost 300 different parts of the skin in these images are cropped and applied on both “Pixel-by-pixel” and “Modified histogram matching” methods. Results are presented in Table 3.2.

Due to the high number of available query images, ten images have been selected randomly from the image set to demonstrate in this study. In this section, the Fitzpatrick scale reference data-set and also Dior cosmetic palette have been both tested on real query images using “Modified histogram matching” and “Pixel-by-Pixel” algorithms. Moreover, a comparison has been made for the results to investigate if there would be any different output for the algorithms.

Table 3.2: The Fitzpatrick real skin image classification Using “Pixel-by-pixel” algorithm



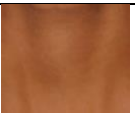
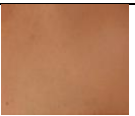



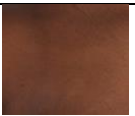

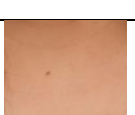
Ref / Query	Class 1	Class 2	Class 3	Class 4	Class 5	Class 6
	✗					
			✗			
					✗	
				✗		
	✗					
			✗			
			✗			
						✗
			✗			
				✗		

Table 3.3: Fitzpatrick real skin image classification using “Modified histogram matching.”









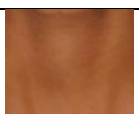




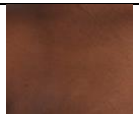


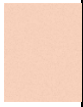
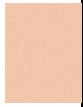











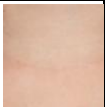
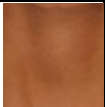
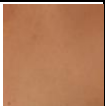
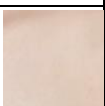

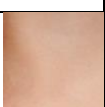
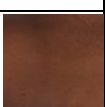

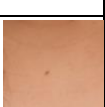
Ref Query	Class 1 	Class 2 	Class 3 	Class 4 	Class 5 	Class 6 
	✗					
			✗			
					✗	
				✗		
	✗					
			✗			
			✗			
						✗
			✗			
					✗	

Table 3.4: Dior palette real skin image classification Using “Pixel-by-pixel” method

Ref	Clas s1	Clas s2	Clas s3	Clas s4	Clas s5	Clas s6	Clas s7	Clas s8	Clas s9	Clas s10	Clas s11	Clas s12
Query												
	X											
		X										
							X					
				X								
	X											
		X										
			X									
									X			
			X									
				X								

Table 3.5: Real skin Dior palette classification using “Modified histogram matching”

Ref	Clas s1	Clas s2	Clas s3	Clas s4	Clas s5	Clas s6	Clas s7	Clas s8	Clas s9	Clas s10	Clas s11	Clas s12
Query												
	✗											
		✗										
							✗					
				✗								
	✗											
		✗										
			✗									
									✗			
			✗									
					✗							

The results for experimental studies on real skin images shows a high-level matching for both “Modified Histogram matching” and “Pixel-by-pixel” algorithms. To investigate more about the success rate of these two methods, another study is done by using skin phantoms. Next part of the study tries to verify which algorithm acts better under conditions.

3.6. Experimental Results on Skin Phantoms for Dior Skin Palette

In this section, three different shades of Dior skin foundations from classes six, eight, and four are selected. The selected foundations are applied on a white paper to provide real skin color. Next, the images of these colors are taken by a phone camera, iPhone 7+, and applied in both “Modified Histogram matching” and “Pixel-by-pixel” algorithms. As shown in Figure 3.15, the “Pixel-by-pixel” algorithms have classified all three colors correctly however, the “Modified Histogram matching” algorithm has classified the third image as class two, while this image belongs to the class four.

Next, a black spot which demonstrates any skin mole is applied on the color papers, as shown in Figure 3.16. Images are taken again by iPhone 7+ and tested by the algorithms. The “Pixel-by-pixel” algorithms provided accurate results for all three classes. The “Modified Histogram matching” algorithm classified images two and three in classes ten and five, however these images have been taken from classes eight and four, respectively.

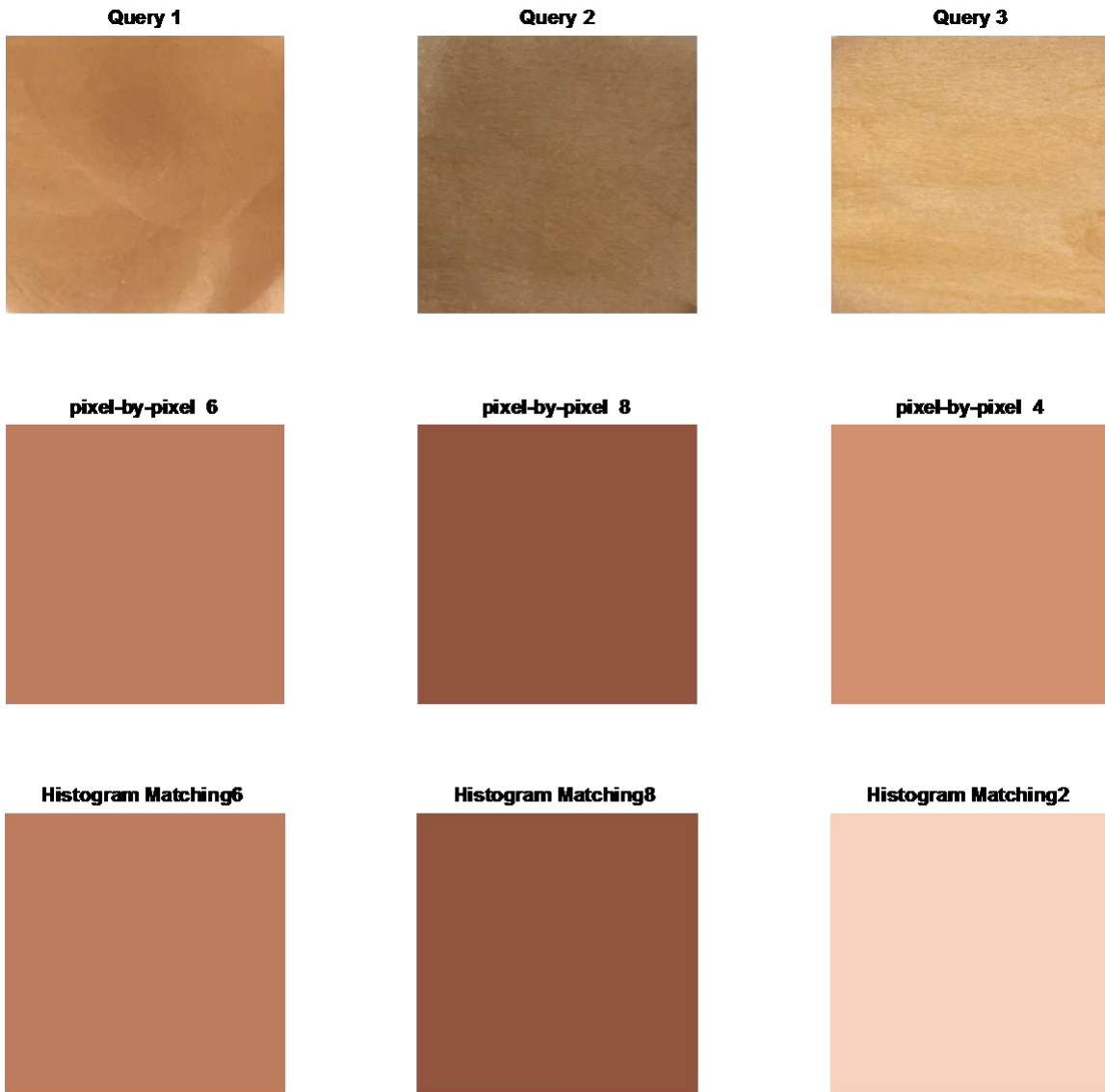


Figure 3.15: Dior skin foundation shades classification based on the Dior palette

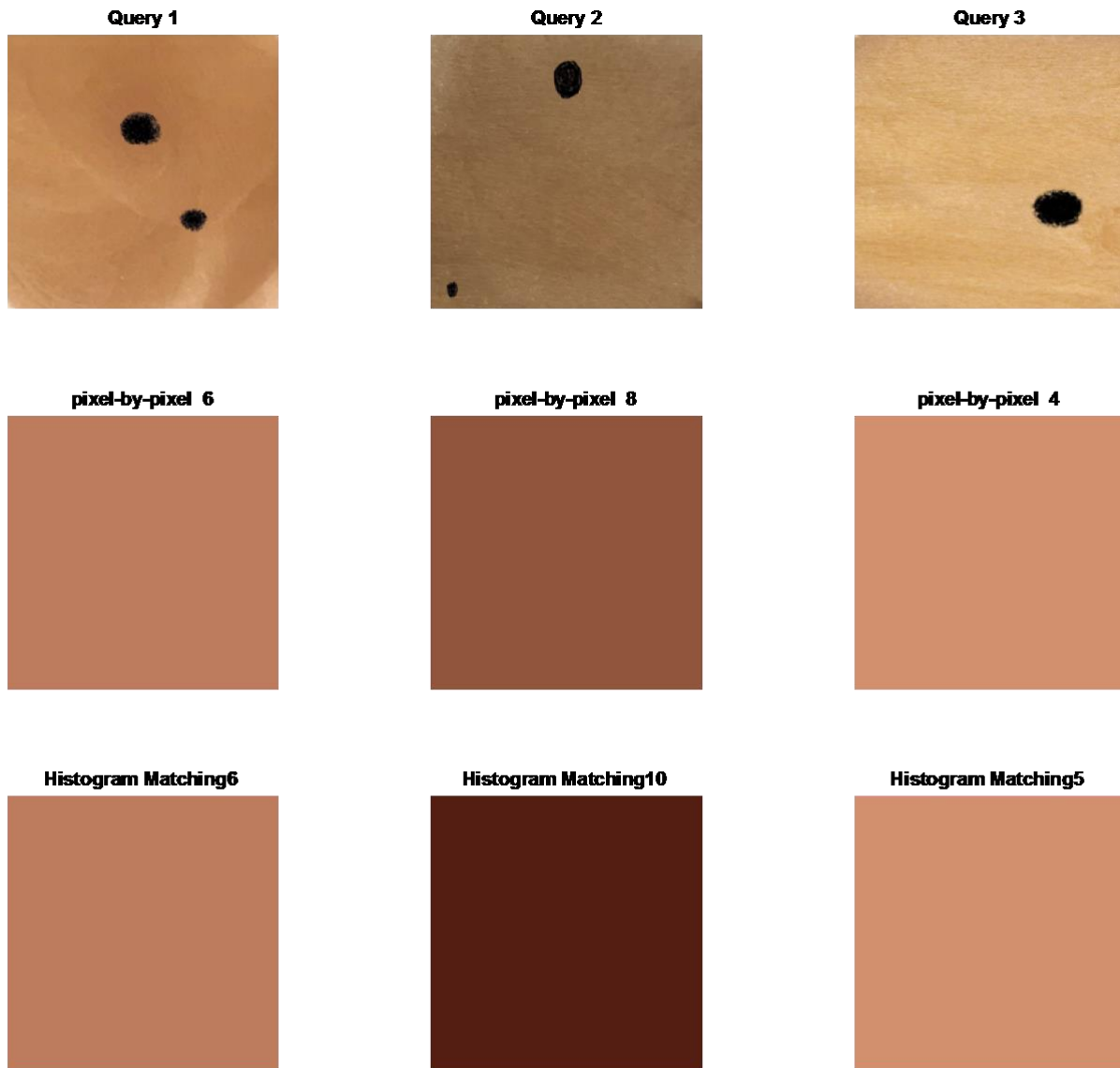


Figure 3.16: Modified Dior skin foundation shades classification based on the Dior palette

3.7. Conclusions

In this chapter, the two main algorithms for color classification, “Pixel-by-Pixel” and “Modified Histogram Matching”, has been tested and verified. As demonstrated, this two algorithms are applied on two types of skin color reference images: The Fitzpatrick skin scale [9] and Dior skin Palette [23]. The validation set is created by perturbing reference image sets. Implementing two methods by two validation image sets, proves the accuracy of these methods. In the next sections, both algorithms are applied on real skin images which are cropped from the real portrait images [29]. Results for both Fitzpatrick skin scale and Dior skin palette are shown in section 3.5. A high matching results is achieved between two applied algorithms.

To investigate more about the accuracy of these methods, three different color foundations from Dior skin Palette are purchased to simulate real skin colors based on the introduced reference set, Dior skin color palette. The experiments on simulated skin colors are done in two different parts, the first part is based on the simulated monotone skin color images and the second part is based on simulated skin images with a dark spot or a mole. From the results of classification in these two parts, we conclude that the “Modified Histogram matching” has a significant weakness in image retrieval applications for skin images specially skins with any dark spot or mole. Based on the simulated skin image classification results which are from a known color in Dior palette, different results obtained by using “Modified Histogram Matching” method.

Chapter 4. Conclusion & Future Works

The purpose of this study is to develop an algorithm which can classify all types of colors into desired reference colors unaccompanied by a human. The algorithms applied in this study are not limited to skin shade images, as all types of color images with different reference images can be implemented using these algorithms. Several methods have been applied in this study to meet the objectives of this study. Due to the similarity of human skin shades, it has been hard to diagnose the color of skin and categorize it into specified reference colors. Thus, our study focused on human skin color detection and classification.

Human skin color detection has always been needed to be classified using the naked eye, which makes it complicated in some applications. Color perception is an astonishingly complicated procedure which can be different between people due to some differences in any one of the areas in human eye biology. These differences are small compared to the number of various colors that human can see, but large enough to cause measurement error [50]. These differences are highly evident in human skin color, which is difficult to distinguish.

Our study applied two different methods to classify human skin color images: “Pixel by Pixel” algorithm as a spatial dependent and “Modified Histogram Matching” algorithm as a spatial independent.

“Pixel by Pixel” algorithm works based on the distance between two images. Several methods for measuring distance between images are introduced in chapter 2. Among the introduced techniques, “Euclidean distance” is chosen as the most straight-forward method for the classification approach of this study.

“Modified Histogram Matching” algorithm is the second method which is proposed in this study. As stated in chapter 2, conventional histogram matching techniques have a chief drawback for images with monotone color. Comparing monotone color image histograms which are only single bars will give invalid results, as single bar histograms can hardly overlap to be classified in a same class. Therefore, “Modified Histogram Matching” provides a method to assign a Gaussian distribution to single bar histograms. Applying this will help to retrieve the most similar image among the adjacent histograms.

In chapter 3, both methods are tested on two different reference images: Fitzpatrick skin scale [9] and Dior skin palette [23]. To validate the proposed algorithms, a validation set is created based on perturbed reference images. Applying the validation set with known results on introduced algorithms, confirms the accuracy of their application. Following this, real skin images which are extracted from portrait images are tested in introduced algorithms. The results for these experiments are shown in section 3.4.

Further experiments are done on Dior skin palette, using three different color foundations of this brand. Three different color foundations are used to simulate skin color using a white monotone surface (a pure white paper). Images of the simulated skin are taken with a phone camera and tested by the algorithms. The experiments demonstrated that the “Pixel by Pixel” algorithm gives more reasonable results.

Another experiment is done by using the simulated skin images with a similar skin mole. This experiment proves the accuracy of the “Pixel-by-Pixel” algorithm. Modified Histogram matching algorithm failed in this experiment. This method, classifies the simulated skin colors in the classes other than classes of the selected foundations.

As developing proper hardware is one of the future goals of this study, the speed of running algorithms is highly important in real-time applications. Running speed is another weakness for “Modified Histogram matching” algorithm, as it runs slower compared to pixel by pixel algorithm. From the studies we have done in this thesis, “Pixel by Pixel” is chosen as the best algorithm for the future application.

Development of a user-friendly software or phone application has been given more priority as a future study. The phone application should be capable of working with the phone camera and would be compatible with all operating systems. At this moment, it would be possible for everyone to download and install the app to their phone and use it for different application.

Designing a camera which minimizes the effect of ambient light is highly notable for future applications. The hardware should be able to cancel any ambient light, so the algorithm works under a specified light. This will provide far more accurate results.

References

- [1] S. E. Janine, B. Mia and S. S. Marilyn, "Making Sense of Skin Color in Clinical Care," vol. 21, no. 4, p. 495– 516, 2012.
- [2] C. Gertrude-E and H. Vincent J, "Human skin pigmentation: melanocytes modulate skin color in response to stress," *The FASEB Journal*, vol. 21, no. 4, pp. 976-994, 2007.
- [3] A. M Shamsul, K. Muhammad Gulam and f. Andan, "Dermatological disease diagnosis using color-skin images," *Machine Learning and Cybernetics (ICMLC)*, vol. 5, 2012.
- [4] N. G. Jablonski, "The evolution of human skin and skin color," *Annu. Rev. Anthropol*, vol. 39, p. 585–623, 2004.
- [5] R. Meys, "Skin pigmentation," *Elsevier*, vol. 45, no. 7, 2017.
- [6] S. Sachdava, "Fitzpatrick skin typing: Applications in dermatology," *J Dermatol Veereol Leprol*, no. 75, pp. 93-6, 2009.
- [7] S. Jonathan, "Digital Image Basics".
- [8] M. Nityanand, J. Ashika and S. Vijayasaradhi, "Shining Light on Skin Pigmentation: The Darker and the Brighter Side of Effects of UV Radiation," *PMC*, vol. 88, no. 5, pp. 1075-1082, 2012.
- [9] R. A. S. A. M. M. Fitzpatrick T.B., "Primary malignant melanoma of the skin: the call for action to identify persons at risk; to discover precursor lesions; to detect early melanomas," *J.M. Elwood (Ed.), Naevi and Melanoma: Incidence, Interrelationships and Implications; Pigment Cell, 1, Basle, Karger*.
- [10] J. Youn, J. Oh, B. Kim, D. Suh, J. Chung, S. Oh, J. Kim and S. Kang, "Relationship between skin phototype and MED in Korean, brown skin," *Photodermatol Photoimmunol Photomed*, vol. 13, pp. 208-211, 1997.
- [11] V. Beral, S. Evans, V. Shaw and G. Milton, "Cutaneous factors related to the risk of malignant melanoma," vol. 109, pp. 165-172, 1983.
- [12] M. Weinstock, "Assessment of sun sensitivity by questionnaire: validity of items and formulation of a prediction rule," *J Clin Epidemiol*, vol. 45, pp. 547-552, 1992.
- [13] M. Little and W. M.E., "Skin and hair reflectance of women with red hair," *Ann Human Biol*, no. 8, pp. 231-241, 1981.
- [14] A. B. Holman CDJ., "Pigmentary traits, ethnic origin, benign nevi, and family history as risk factors for cutaneous malignant melanoma," *J Natl Cancer Inst*, vol. 72, pp. 257-266, 1984.
- [15] J. Feather, R. K.S., J. Dawson, J. Cotterill, D. Barker and D. Ellis, "Reflectance spectrophotometric quantification of skin color changes induced by topical corticosteroid preparations," *Br J Dermatol*, vol. 106, pp. 437-444, 1982.
- [16] H. H., F. S.E., G. R.W., M. D.J., S. J.C. and S. B.M., "Do pyridine dimer yields correlate with erythema induction in human skin irradiated in situ with ultraviolet light (275–365 nm)?" *Photochem Photobiol*, vol. 53, pp. 559-563, 1991.
- [17] N. Kollias and A. Baqer, "Spectroscopic characteristics of human melanin in vivo," *J Invest Dermatol*, no. 8, pp. 529-541, 1985.

- [18] F. Susan and M. Antonia, "Surveillance, Race, Culture," *Springer*, 2018.
- [19] R. Gaber, G. Yanina and R. June, "Accuracy of Self-report in Assessing Fitzpatrick Skin Phototypes I Through VI," *JAMA Dermatology*, vol. 149, no. 11, pp. 1282-1294, 2013.
- [20] P. MA, "In memory of Thomas Bernhard Fitzpatrick," *J Invest Dermatol*, vol. 122, no. 2, 2004.
- [21] D. I. John, J. Stuart, A.-O. Alexandra and S. Timothy, "UV Radiation and the Skin," *International Journal of Molecular Sciences*, pp. 12222-12248, 2013.
- [22] M. Douglas S, C. Camille Z, L. Garvey F and F. Mary J, *The Source of the River: The Social Origins of Freshmen at America's Selective Colleges and Universities*, Princeton University Press, 2003.
- [23] D. S. Massey and A. M. Jennifer, "The NIS Skin Color Scale," 2003.
- [24] "Dior Cosmetic," 2019. [Online]. Available: https://www.dior.com/en_int/makeup/complexion/foundation. [Accessed June 2019].
- [25] P. Lynn K, T. Vidyanath P, N. Joel L, C. Judy L, L. Anne G, M. Laurence J and L. Sancy A, "Reflectance Spectrophotometer: The Dermatologists' Sphygmomanometer for Skin Phototyping?," *Journal of Investigative Dermatology*, vol. 128, no. 7, pp. 163-1640, 2008.
- [26] E. Thibodeau and J. D'Ambrosia, "yeasurement of lip and skin pigmentation using reflectance spectraphotometry," *EUROPEAN JOURNAL OF ORAL SCIENCES*, vol. 105, pp. 373-375, 1997.
- [27] R. Luisa, D. Antonio, G. Andrea and P. Carmelo, "Evaluation of the effect of topical agents on radiation-induced skin disease by reflectance spectrophotometry," *Journal of Pharmacy and Pharmacology*, vol. 62, pp. 779-785, 2010.
- [28] T. S, W. W, I. S and L. J, "Noninvasive techniques for the evaluation of skin color.," *J Am Acad Dermatol*, vol. 54, no. 5, 2006.
- [29] C. T. Susan, A. Stéphanie and C. Janusz, "The Taylor Hyperpigmentation Scale: A new visual assessment tool for the evaluation of skin color and pigmentation," *cutaneous medicine for the practitione*, vol. 76, no. 4, 2005.
- [30] A. Dass', 2019. [Online]. Available: <https://www.angelicadass.com/humanae-project>.
- [31] "<http://www.cambridgeincolour.com/tutorials/color-spaces.htm>," [Online].
- [32] B. Dibya Jyoti, A. K. Gupta and A. K. Fayaz, "Comparing the Performance of L*A*B* and HSV Color Spaces with Respect to Color Image Segmentation," *International Journal of Emerging Technology and Advanced Engineering*, vol. 5, no. 2, 2015.
- [33] P. Baldelli and M. Paciella, "Creation and implementation of a pressure ulcer prevention bundle improves patient outcomes," *American Journal of Medical Quality*, vol. 23, no. 2, pp. 136-142, 2008.
- [34] M. D. Fairchild, "Color appearance models," *Hoboken, NJ: Wiley*, 2005.
- [35] H. Lee, *Introduction to color imaging science*, Cambridge, UK: Cambridge University Press., 2005.
- [36] J. Z. A. d. M. C. C. Samia Aïnouz, "Physical interpretation of polarization-encoded images by color preview," *Optics Express*, vol. 14, no. 13, pp. 5916-5927.

- [37] F. Myron, S. Harpreet, N. Wayne, A. Jonathan, H. Qian, D. Byron, G. Monika, H. Jim, L. Denis, P. Dragutin, S. David and Y. Pater, "Query by image and video content," *IEEE Computer*, vol. 28, no. 9, p. 23–32, 1995.
- [38] J. R. Bach, C. Fuller, A. Gupta, A. Hampapur, B. Horowitz, R. Humphrey, R. C. Jain and C. Shu, "an open framework for image management," *In Symposium on Electronic Imaging: Science and Technology - Storage and Retrieval for Image and Video Databases IV*, pp. 76-87, 1996.
- [39] O. Virginia and S. Michael, "Retrieval from a relational database of images," *IEEE Computer*, vol. 28, no. 9, pp. 40-48, 1995.
- [40] S. Michael and B. Dana, "Color indexing," *International Journal of Computer Vision*, pp. 11-32, 1991.
- [41] P. Greg and Z. Ramin, "Histogram refinement for content-based image retrieval," *IEEE Workshop on Applications of Computer Vision*, pp. 96-102, 1996.
- [42] S. M. J and B. D. H, "Indexing via color histograms," *Proceedings of the 3rd International Conference on Computer Vision*, pp. 390-393, 1990.
- [43] S. M.J and B. D.H, "Color indexing," *International Journal of Computer Vision*, pp. 11-32.
- [44] W. C.-H. C. a. L.-M. P. K.-M, "Merged-color histogram for color image retrieval.," *Proceedings of the 2002 International Conference on Image Processing*, vol. 3, p. 949–952, 2002.
- [45] G. Borgefors, "Applications using distance transforms," *Aspects of Visual Form Processing*, pp. 83-108, 1994.
- [46] B. R and D. T, "A COMPARISON STUDY ON METHODS FOR MEASURING DISTANCE IN IMAGES," *International Journal of Research in Computers*, 2012.
- [47] E. Castillo, A. Hadi, N. Balakrishnan and J. Sarabia, "Extreme Value and Related Models with Applications in Engineering and Science," *John Wiley & Sons*, 2005.
- [48] M. Davis and P. Edberb, Google, Apple, [Online]. Available: <http://www.unicode.org/reports/tr51/#Diversity>.
- [49] Adobe, "photoshop," 19 02 1990. [Online]. Available: <https://www.photoshop.com/>.
- [50] S. K. Shevell, "Color Appearance," in *The Science of Color*, 2003.
- [51] "Skin reflectance spectrophotometry.," *photo-Dermatology*, vol. 4, no. 3, pp. 167-71, 1987.
- [52] L. Ian and D. Bernard, "Skin Color Measurements in Terms of CIELAB Color Space Values," *Journal of Investigative Dermatology*, vol. 99, no. 4, pp. 468-473, 1992.
- [53]
- [54] J. Davidoff, *Cognition Through Color*, MIT Pres, 1991.
- [55] A. Green, *Colour Questions: What? Where? Who? Why? How?*, 5 Congreso Argentino del Color, 2002, pp. 125-138.
- [56] F. Taylor, *Colour Technology for Artists, Craftsmen, and Industrial Designers*, Oxford University Press, 1962.
- [57] B. Robertson, "Like in the Movies," *Computer Graphic World*, 2004.
- [58] C. Poynton, "A Guided Tour of Color Space," in *New Foundations for Video Technology (Proceedings of the SMPTE Advanced Television and Electronic Imaging Conference)*, San Francisco, 1996.

- [59] J. W, Z. H, H. X and W. and Q, "Symmetric colour ratio gradients in spiral architecture," *Proceedings of the 18th International Conference on Pattern Recognition*, pp. 204-213, 2006.
- [60] D. Tobi, M. Kevan, L. Shih-Chii, L.-B. Bernabé and P. M. Diederik, "Analog And Digital Implementations Of Retinal Processing For Robot Navigation Systems," ETH Zurich, 2016.
- [61] L. Wenjuan, J. Jianlin, H. Chen and Y. Chenyu, "Optimal Color Design of Psychological Counseling Room by Design of Experiments and Response Surface Methodology," *PLOS ONE*, vol. 9, no. 3, 2014.
- [62] B. Milton E and N. Dorothy, "Color-Order Systems, Munsell and Ostwald," *Journal of the Optical Society of America*, vol. 32, no. 12, pp. 709-719, 1942.